

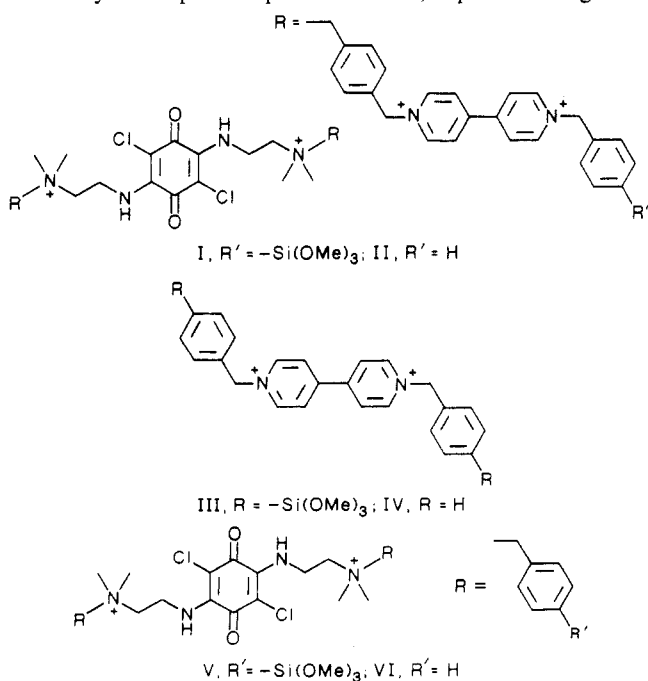
Charge-Transport Properties of an Electrode-Confined Redox Polymer Derived from a Monomer Consisting of a Quinone Flanked by Two Benzylviologen Subunits

Diane K. Smith, Gregg A. Lane, and Mark S. Wrighton*

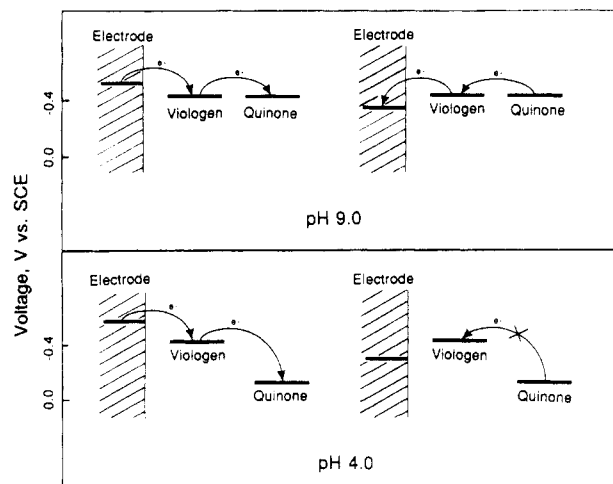
Department of Chemistry, Massachusetts Institute of Technology, Cambridge, Massachusetts 02139
(Received: October 16, 1987)

Electrochemical and optical spectroelectrochemical characterization of an electrode-confined siloxane-based polymer having two benzylviologen subunits flanking a benzoquinone subunit is reported. The polymer, $(\text{BV-Q-BV}^{6+})_n$, is formed by hydrolysis of the $-\text{Si}(\text{OMe})_3$ groups of the monomer I, 1,1''-[2,5-dichloro-3,6-dioxo-1,4-cyclohexadiene-1,4-diyl]bis[imino-2,1-ethanediyldimethyliminio)methylene-1,4-phenylenemethylene]bis[1'-[[4-(trimethoxysilyl)phenyl]methyl]-4,4'-bipyridinium. Further, electrochemical and optical properties of the solution analogue of I are reported. The (BV-Q-BV^{6+}) unit has two fixed positive charges, one in each of the BV-Q links. The (BV-Q-BV^{6+}) unit is reducible by a $6e^-/2\text{H}^+$ process in a manner roughly consistent with the behavior of BV^{2+} ($E^\circ(\text{BV}^{2+/+}) \approx -0.5$ V vs SCE; $E^\circ(\text{BV}^{+/0}) \approx -0.9$ V vs SCE) and Q ($E^\circ(\text{Q}/\text{QH}_2) \approx -0.3$ V vs SCE at pH 7) studied separately in solution and as siloxane-based polymers confined to electrodes. The important finding is that the $(\text{BV-Q-BV}^{6+})_n$ system shows pH-dependent rectification in the sense that at low pH, less than ~ 6 , the reduction of the Q centers to QH_2 cannot be electrochemically reversed, even at electrode potentials significantly positive of $E^\circ(\text{Q}/\text{QH}_2)$. Thus, reducing equivalents can be kinetically and thermodynamically trapped in the form of QH_2 . The rectification observed is established to be due to a combination of kinetic, thermodynamic, and structural factors all consistent with the conclusion that reduction of all Q centers to QH_2 occurs via reducing equivalents delivered through the $\text{BV}^{2+/+}$ system and that the reverse process is possible only above a certain pH, ≥ 6 . Studies of conventional electrode-confined bilayers $(\text{BV}^{2+})_n/(\text{Q})_n$ and electrode-confined $(\text{Q})_n$ are reported and reveal factors influencing the rectification in $(\text{BV-Q-BV}^{6+})_n$: charge transport in $(\text{Q})_n$ via Q/QH_2 self-exchange is very sluggish but reduction of Q to QH_2 via BV^+ can be fast. Previous studies of $(\text{BV}^{2+/+})_n$ show that charge transport via $\text{BV}^{2+/+}$ self-exchange can be fast and is pH-independent, but steady-state charge transport via $\text{BV}^{2+/+}$ self-exchange in $(\text{BV-Q-BV}^{6+})_n$ is significantly slower and is modestly pH dependent in a manner consistent with cross exchange between the $\text{BV}^{2+/+}$ and Q/QH_2 contributing to charge transport at pH ≥ 6 but not for pH < 6 . The temperature dependence of steady-state charge transport in $(\text{BV-Q-BV}^{6+})_n$ shows an Arrhenius activation energy of 50–60 kJ/mol.

In this article we elaborate the characterization¹ of electrode-confined redox polymer, $(\text{BV-Q-BV}^{6+})_n$, derived from the monomer I, by hydrolysis of the $-\text{Si}(\text{OMe})_3$ groups.² We also report the solution electrochemistry and optical spectral properties of the nonpolymerizable analogue II. Electrochemistry of electrode-confined polymers from III, $(\text{BV}^{2+})_n$, and solution electrochemistry of its nonpolymerizable analogue, IV, have been reported previously,¹ providing data for one of the redox subunits in I and II. In this article we include aspects of the electrochemistry of the quinone species V and VI, to provide background



SCHEME I: Representation of the pH Dependence of the Electrochemical Behavior of $(\text{BV-Q-BV}^{6+})_n$



information regarding the quinone subunit in I and II. The interesting properties of II and $(\text{BV-Q-BV}^{6+})_n$ stem from the fact that these materials consist of two different kinds of redox subunits. The benzylviologen centers, BV^{2+} , are known to be one-electron redox systems with pH-independent E° values at ~ -0.5 ($\text{BV}^{2+/+}$) and -0.9 ($\text{BV}^{+/0}$) V vs SCE,^{3,4} whereas the quinone center Q is a two-electron, two-proton, pH-dependent redox center, with E°

(1) Smith, D. K.; Lane, G. A.; Wrighton, M. S. *J. Am. Chem. Soc.* **1986**, *108*, 3522.

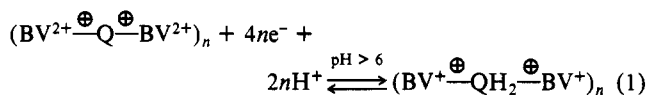
(2) Murray, R. W. *Electroanal. Chem.* **1984**, *13*, 191, and references therein.

(3) (a) Dominey, R. N.; Lewis, T. J.; Wrighton, M. S. *J. Phys. Chem.* **1983**, *87*, 5345. (b) Lewis, T. J.; White, H. S.; Wrighton, M. S. *J. Am. Chem. Soc.* **1984**, *106*, 6947. (c) Lewis, T. J. Ph.D. Thesis, Massachusetts Institute of Technology, 1984.

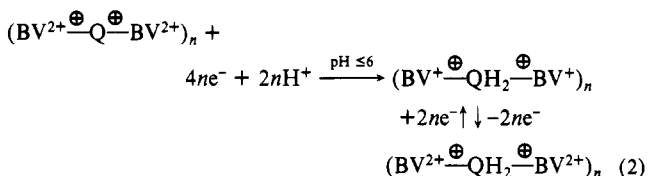
(4) Bookbinder, D. C.; Wrighton, M. S. *J. Electrochem. Soc.* **1983**, *130*, 1080.

* Address correspondence to this author.

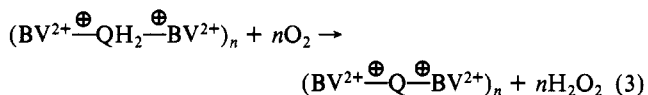
= -0.3 V vs SCE at pH 7 (Q/QH₂). Preliminary characterization of electrode-confined (BV-Q-BV⁶⁺)_n in aqueous electrolytes has shown that the electrochemistry is pH-dependent. For high pH's there is a "reversible" 4ne⁻/2nH⁺ redox system, eq 1, where each



BV²⁺ center is reduced by one electron and each Q center is reduced by 2e⁻/2H⁺. Note that I and II have two fixed positive charges associated with the linkage between the Q and BV²⁺ centers. For low pH's (6 or below) the 4ne⁻/2nH⁺ reduction of (BV-Q-BV⁶⁺)_n occurs, but only the electrons added to the BV²⁺ centers can be removed electrochemically. Thus, charge is "trapped" in the polymer in the form of the reduced quinone centers, QH₂, (2). The electrochemical characterization shows



that (BV-QH₂-BV⁶⁺)_n is not oxidizable even at potentials significantly positive of E^o(Q/QH₂). Chemical oxidation of the QH₂ centers can occur as illustrated by reaction with O₂, (3). The



rationale for the pH-dependent rectification is that at low pH's E^o(BV²⁺+/) is much more negative than E^o(Q/QH₂), making the reduction of Q by BV⁺ so far thermodynamically downhill that the reverse process is very slow and effectively does not occur. Apparently, the (BV-Q-BV⁶⁺)_n polymer does not transport charge among the Q centers; reduction of Q to QH₂ occurs via delivery of charge from the BV⁺ centers. Empirically, at low pH's where E^o(BV²⁺+/) is much more negative than E^o(Q/QH₂) the Q redox centers are not directly accessible, presumably because the Q/QH₂ system in the (BV-Q-BV⁶⁺)_n polymer has a negligible charge-transport rate. The structure and composition of the polymer, the slow kinetics for Q/QH₂ self-exchange,⁵ and the thermodynamics at low pH are all likely contributors to the ability to put charge into the (BV-Q-BV⁶⁺)_n and being unable to electrochemically extract the charge from the QH₂ centers. Scheme I illustrates the pH dependence of "rectification" that is found with electrode-confined (BV-Q-BV⁶⁺)_n.

The results for (BV-Q-BV⁶⁺)_n indicate that the polymer behaves as if it were a bilayer assembly consisting of an inner layer (nearest the electrode) of (BV²⁺)_n and an outer layer (nearest the electrolyte solutions) of (Q)_n like the bilayer assemblies reported first by Murray.⁶ Recently, Meyer has reported a polymer bilayer assembly where the outer layer has a pH-dependent E^o.⁷ In the system reported here, Scheme I, the charge trapping occurs throughout the polymer, and the (BV-Q-BV⁶⁺)_n is thus a "homogeneous bilayer". There have been previous reports of "mixed" redox polymers formed by copolymerization of different monomers.^{8,9} In such cases the consequences of concentration

dilution on charge-transport rate has been found to be a diminution in rate, as expected. However, though rectification of the sort indicated in Scheme I in such a system is, in principle, possible, the system represented by (BV-Q-BV⁶⁺)_n is unique, because charge transport via the Q/QH₂ system, even when pure (as for the polymer from V), is slow. The point is that the BV²⁺+/+ system represents the principal path for charge transport to and from the Q centers. The (BV-Q-BV⁶⁺)_n system behaves as if the BV²⁺+/+ system plays the role of a mobile redox mediator as has been reported for other polymer systems.⁹⁻¹¹ Since the reduction of the Q centers to the QH₂ state can apparently be irreversible at low pH, the kinetics for quinone self-exchange are known to be pH-dependent,⁵ and the energetics and kinetics for the cross reaction represented by (4) are expected to be pH-dependent, we



include here the results of a study of the pH dependence of the steady-state charge transport in electrode-confined (BV-Q-BV⁶⁺)_n.

Experimental Section

Materials and General Equipment. Chemicals used in the syntheses were prepared as follows: HPLC-grade CH₃CN was distilled over P₂O₅ and then run through a column of activated Al₂O₃. Reagent-grade Me₂SO was stirred over CaH₂ and then distilled in vacuo. 4,4'-Bipyridine (Kodak) was purified by sublimation or recrystallization from CH₃CN. α,α'-Dibromo-p-xylene (Aldrich) was recrystallized from acetone. Benzyl chloride (Aldrich) was run through a column of activated Al₂O₃, and p-(trimethoxysilyl)benzyl chloride (Petrarch) was distilled in vacuo. Electrolytes and buffer materials were used as received from commercial sources and showed negligible electrochemically active impurities for the potential range of interest.

¹H NMR spectra were recorded on a Varian 60-MHz spectrometer, a Jeol 90-MHz FT spectrometer, or a Bruker 250-MHz FT spectrometer. Absorption spectra were recorded on a HP 8451A diode array spectrometer. Elemental analyses were performed by Galbraith Laboratories, Nashville, TN.

Synthesis of 2,5-Dichloro-3,6-bis[2-(dimethylamino)ethyl]-amino-1,4-benzoquinone (VII). This quinone was synthesized by a previously reported procedure for the 3-(dimethylamino)propylamine analogue.¹² Samples of 14.6 g of tetrachloro-1,4-benzoquinone, 21.2 g of 2-(dimethylamino)ethylamine, and 200 mL of 1,4-dioxane were combined, and the mixture was heated at 100 °C in an oil bath for 6 h. The reaction mixture was then concentrated in vacuo, and the precipitate was collected by vacuum filtration. Recrystallization from EtOH yielded 13.9 g of bright red needles: ¹H NMR (90 MHz, CDCl₃) δ 7.95 (br s, 1 H), 4.7 (d of d, 2 H), 2.65 (t, 2 H), 2.35 (s, 6 H). Anal. Calcd (Found) for C₁₄H₂₂Cl₂N₄O₂: C, 48.15 (47.99); H, 6.35 (6.38); N, 16.04 (15.99); Cl, 20.30 (20.25).

Synthesis of N-Phenylmethyl-4,4'-bipyridinium (VIIIa) and N-[4-(Trimethoxysilyl)phenyl]methyl-4,4'-bipyridinium (VIIIb). The monoalkylated bipyridines were synthesized by dissolving 4,4'-bipyridine in neat benzyl chloride or p-(trimethoxysilyl)benzyl chloride and warming for 2 h in a 50 °C oil bath, to form VIIIa or VIIIb, respectively. In a typical procedure, 0.5 g of 4,4'-bipyridine and 10 mL of benzyl chloride were used. The white solid which precipitated was collected by vacuum filtration and washed with tetrahydrofuran to give 0.77 g (85%) of VIIIa. The dialkylated bipyridinium does not form under the reaction conditions used, presumably due to the insolubility of the desired monoalkylated species in the reaction medium. Spectral data were as follows: ¹H NMR (250 MHz, D₂O) δ 8.74 (d, 2 H), 8.44 (d, 2 H), 8.10 (d, 2 H), 7.59 (d, 2 H), 7.24 (s, 5 H), 5.58 (s, 2 H). The yield of VIIIb was similar, and VIIIb was characterized by ¹H NMR (250 MHz, D₂O) δ 8.78 (d, 2 H), 8.52 (d, 2 H), 8.17 (d,

(5) Laviron, E. *J. Electroanal. Chem.* **1984**, *169*, 29; *J. Electroanal. Chem.* **1986**, *208*, 357.

(6) (a) Pickup, P. G.; Murray, R. W. *J. Electrochem. Soc.* **1984**, *131*, 833. (b) Pickup, P. G.; Kutner, W.; Leidner, C. R.; Murray, R. W. *J. Am. Chem. Soc.* **1984**, *106*, 1991. (c) Abruna, H. D.; Denisevich, P.; Umana, M.; Meyer, T. J.; Murray, R. W. *J. Am. Chem. Soc.* **1981**, *103*, 1. (d) Denisevich, P.; William, K. W.; Murray, R. W. *J. Am. Chem. Soc.* **1981**, *103*, 4727.

(7) Vining, W. J.; Surridge, N. A.; Meyer, T. J. *J. Phys. Chem.* **1986**, *90*, 2281.

(8) Murray, R. W.; Facci, J. S.; Schmehl, R. H. *J. Am. Chem. Soc.* **1982**, *104*, 4959.

(9) Buttry, D. A.; Anson, F. C. *J. Am. Chem. Soc.* **1984**, *106*, 59.

(10) Fukui, C. M.; Degrand, C.; Miller, L. L. *J. Am. Chem. Soc.* **1982**, *104*, 28.

(11) Anson, F. C.; Ni, S.-L. *J. Am. Chem. Soc.* **1985**, *107*, 3442.

(12) Cavallito, C. J.; Soria, A. E.; Hoppe, J. A. *J. Am. Chem. Soc.* **1950**, *72*, 2662.

2 H), 7.68 (d, 2 H), 7.55 (d, 2 H), 7.29 (d, 2 H), 5.65 (s, 2 H), 3.10 (s, 9 H).

Synthesis of *N*-[4-(Bromomethyl)phenyl]methyl-*N'*-phenylmethyl-4,4'-bipyridinium (IXa) and *N*-[4-(Bromomethyl)phenyl]methyl-*N'*-[4-(trimethoxysilyl)phenyl]methyl-4,4'-bipyridinium (IXb). The benzylviologen derivatives were prepared by reacting VIIIa or VIIIb with a 2-fold excess of α, α' -dibromo-*p*-xylene in CH_3CN . For 0.5 g of VIIIa, 1 g of dibromoxylene and 20 mL of CH_3CN were used. The mixture was refluxed for 3 h, and the resultant bright yellow precipitate was collected by vacuum filtration and washed with CH_3CN to give 0.90 g (93%) of IXa. In order to obtain reasonable concentrations in CD_3CN , NMR samples of IXa and IXb were prepared as the PF_6^- salt by adding excess NH_4PF_6 , precipitating NH_4X (X = Cl, Br). NMR spectra were as follows: IXa: ^1H NMR (60 MHz, CD_3CN) δ 8.83 (d, 4 H), 8.23 (d, 4 H), 7.41 (s, 9 H), 5.74 (s, 4 H), 4.53 (s, 2 H). IXb: ^1H NMR (250 MHz, CD_3CN) δ 8.99 (d, 4 H), 8.39 (d, 4 H), 7.74 (d, 2 H), 7.53 (m, 6 H), 5.86 (s, 2 H), 5.83 (s, 2 H), 4.62 (s, 2 H), 3.60 (s, 9 H).

Synthesis of I and II. Two equivalents of IXa or IXb and 1 equiv of VII were dissolved in Me_2SO . For 0.143 g of VII, 0.448 g of IXa and 20 mL of Me_2SO were used. The solution was heated for 3 h in a 70 °C oil bath. After cooling, tetrahydrofuran was added to precipitate a rust-colored solid. This solid was washed with copious amounts of tetrahydrofuran and/or CH_3CN to give 0.41 g (69%) of II.

For analytical purposes II was converted to the PF_6^- salt by adding a >10-fold excess of NH_4PF_6 to a suspension of II in CH_3CN . The PF_6^- salt of II gradually dissolves, turning the solution pink, and white NH_4X (X = Cl, Br) precipitates. The mixture was filtered and the filtrate evaporated to yield a light rust-colored powder, which is not hygroscopic. ^1H NMR (250 MHz, CD_3CN) δ 8.96 (d of d, 4 H), 8.39 (d of d, 4 H), 7.63 (s, 4 H), 7.51 (s, 5 H), 7.06 (br s, 1 H), 5.88 (s, 2 H), 5.83 (s, 2 H), 4.49 (s, 2 H), 4.26 (m, 2 H), 3.55 (m, 2 H), 3.01 (s, 6 H). Anal. Calcd (Found) for $\text{C}_{64}\text{H}_{68}\text{Cl}_2\text{F}_{36}\text{N}_8\text{O}_2\text{P}_6$: C, 40.00 (39.71); H, 3.57 (3.46); Cl, 3.69 (3.81); F, 35.58 (34.49); N, 5.83 (6.07).

A sample of I was prepared in the same manner as for II and characterized by ^1H NMR (250 MHz, CD_3CN) δ 8.98 (m, 4 H), 8.40 (m, 4 H), 7.74 (d, 2 H), 7.64 (s, 4 H), 7.55 (d, 2 H), 5.88 (s, 2 H), 5.84 (s, 2 H), 4.50 (s, 2 H), 4.28 (m, 2 H), 3.59, 3.56, 3.58 (overlapping s, s, and m, 11 H), 3.02 (s, 6 H), 2.58 (s, Me_2SO).

Synthesis of V and VI. The quinone derivatives V and VI were prepared by reacting VII with excess benzyl chloride or *p*-(trimethoxysilyl)benzyl chloride in refluxing CH_3CN to give VI or V, respectively. The rust-colored precipitate was collected by vacuum filtration. Spectral data were as follows: V: ^1H NMR (250 MHz, CD_3CN) δ 7.63 (d of d, 4 H), 4.45 (s, 2 H), 4.22 (br s, 2 H), 3.59 (s, 9 H), 3.50 (m, 2 H), 2.99 (s, 6 H). VI: ^1H NMR (250 MHz, CD_3OD) δ 7.56 (m, 5 H), 4.65 (s, 2 H), 4.32 (t, 2 H), 3.67 (t, 2 H), 3.14 (s, 6 H).

Electrodes. Pt flag electrodes were prepared from 0.2-mm Pt sheet and pretreated prior to derivatization as described elsewhere.¹³ SnO_2 electrodes were fabricated from SnO_2 -coated glass generously provided by Dr. David L. Morse of Corning Glass Works, Corning, NY. These were cleaned before derivatization by sonicating for 15 min in PEX/ H_2O and then rinsing with H_2O .

Fabrication of the eight-electrode microelectrode arrays used in this study has been previously described.¹⁴ Basically, photolithographic procedures are used to produce arrays of eight, $\sim 50 \mu\text{m}$ long $\times \sim 2 \mu\text{m}$ wide $\times 0.1 \mu\text{m}$ high Au microelectrodes on a Si_3N_4 -coated Si/ SiO_2 substrate. These electrodes are separated by $\sim 1.4 \mu\text{m}$ and are individually electrically contacted. The leads to the electrodes are covered with clear epoxy (Hysol), and the "chips" are mounted on a gold header. Connections from the header to the chip are made with silver epoxy, and the leads are

covered with white epoxy (Hysol). Electrodes are cleaned prior to use first by a 1-min O_2 plasma etch at 300 W forward power and second by a negative potential excursion to give H_2 evolution in aqueous electrolyte. Pt was electrodeposited onto the microelectrodes from a solution containing 2 mM K_2PtCl_6 and 0.1 M K_2HPO_4 to produce a fresh electrode surface and also to close the spacings between electrodes to $\sim 0.3 \mu\text{m}$. The electrodes were characterized before derivatization by examining the electrochemical response in a 5 mM solution of $\text{Ru}(\text{NH}_3)_6\text{Cl}_3$ which reveals a sigmoidal current-voltage curve characteristic of microelectrodes.¹⁵ Electrochemical testing is carried out to establish that only the microelectrode array (and not leads or contact pads) are exposed to electrolyte solution.

Electrode Derivatization. Electrodes were derivatized with $(\text{BV-Q-BV}^{6+})_n$ by potentiostating at -0.7 V vs SCE in a 5 mM solution of I in aqueous 0.2 M KCl/0.1 M K_2HPO_4 until the desired coverage was achieved. After derivatization the electrodes were stored in 0.5 M KCl/pH 7.2 buffered solutions. Coverage was determined by integration of cyclic voltammetry waves at pH 7.2 and at sweep rates low enough to accurately reflect actual coverage.

Electrochemical Equipment and Procedures. Electrochemical experiments were performed by using either a PAR Model 363 potentiostat/galvanostat and PAR Model 175 universal programmer with a Houston Instruments Model 2000 *x-y* recorder, or a Pine Model RDE4 bipotentiostat coupled with a Kipp and Zonen BD91 *x-y-y'* recorder. The current-time response for the chronoamperometry experiments was recorded with a Tektronix Type 549 storage oscilloscope.

All electrochemical experiments were carried out under N_2 or Ar by using a standard three electrode configuration with a Pt counter electrode and saturated calomel (SCE) reference. All experiments were done in a one-compartment cell, except for bulk electrolysis of VI to produce QH_2 , which was done in a two-compartment cell with a high surface area Pt gauze working electrode. Spectroelectrochemical measurements were made in a quartz cuvette with a derivatized SnO_2 electrode as the working electrode. The pH 9, 8, and 7.2 electrolyte solutions were buffered with 0.1 M tris(hydroxymethyl)aminomethane/HCl (Tris/Tris-HCl) and the pH 6, 5, and 4 solutions were buffered with 0.1 M $\text{Na}[\text{CH}_3\text{COO}]/\text{CH}_3\text{COOH}$. Solutions of 0.1 M H_2SO_4 and 0.5 M NaHSO_4 were used for pH 1 experiments. Experiments at pH 3 were carried out with 0.05 M KH_2PO_4 buffer adjusted with 0.1 M HCl.

Thickness Measurements. Thicknesses of $(\text{BV-Q-BV}^{6+})_n$ at different coverages were obtained with a Sloan Dektak surface profile measuring system. Electrodes were prepared according to previously published procedures.^{3b} To produce a "step" across which the stylus of the surface profiler is drawn, Apiezon N grease was applied to part of the electrode surface and then removed with CH_2Cl_2 after derivatization.

Scanning Electron Microscopy. The microelectrode arrays and Au-coated glass electrodes used to establish thickness were examined by electron microscopy using a Cambridge Mark 2A Stereoscan with a resolution of 20 nm. Samples were first coated with about 200 Å of Au to minimize problems from surface charging.

Rotating Disk Experiments. The determination of fast electron transfer rates at polymer-modified rotating microelectrodes has recently been described.¹⁶ Briefly, a 25- μm Pt wire is embedded in clear epoxy (Dexter Corp., Hysol Division) such that a cross section of the wire is exposed on the electrode surface near the edge of a 1-cm-diameter disk. The Pt microelectrode is exposed by polishing and is off-center. For the particular microelectrode assembly using in this work, rotation at a given rotation velocity was shown to give an effective $\omega^{1/2}$ 5.0 times larger than for a conventional rotating disk electrode. The details of this procedure are in ref 16. The microelectrodes were derivatized with $(\text{BV}^{2+})_n$

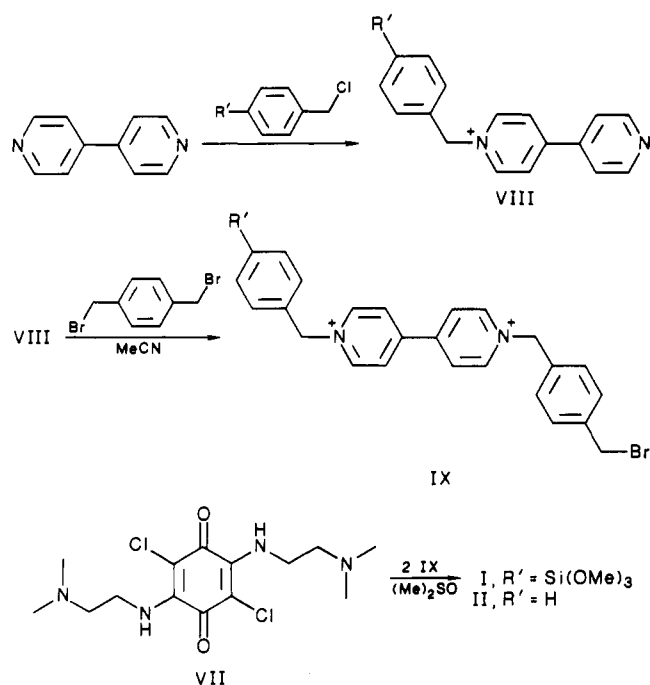
(13) Lenhard, J. R.; Murray, R. W. *J. Electroanal. Chem.* **1977**, *78*, 195.

(14) (a) Kittlesen, G. P.; White, H. S.; Wrighton, M. S. *J. Am. Chem. Soc.* **1984**, *106*, 7839; *J. Am. Chem. Soc.* **1985**, *107*, 7373. (b) Thackeray, J. W.; White, H. S.; Wrighton, M. S. *J. Phys. Chem.* **1985**, *89*, 5133. (c) Kittlesen, G. P. Ph.D. Thesis, MIT, 1985.

(15) Howell, J. O.; Wightman, R. M. *Anal. Chem.* **1984**, *56*, 524.

(16) Mallouk, T. E.; Cammarata, V.; Crayston, J. A.; Wrighton, M. S. *J. Phys. Chem.* **1986**, *90*, 2150.

SCHEME II: Synthetic Scheme for the Preparation of Compounds I and II



as previously described^{3b} and then immersed in 0.1 M KCl solutions buffered to pH 5.0 (Na[CH₃COO]/CH₃COOH) containing 0.2–1 mM concentrations of Q.

Results and Discussion

Synthesis of I and II. The details of the synthesis of I and II are given in the Experimental Section. Scheme II summarizes the sequence of reactions leading to the three redox subunit monomer I and its nonpolymerizable analogue II. While the structure is at first forbidding, the molecules can be prepared from commercially available reagents with only one reaction type: displacement of halide from a carbon center by an organic nitrogen compound. The preparation of the compounds is thus straightforward. Since I is hydrolytically unstable by virtue of the two –Si(OMe)₃ groups, the material must be stored under anhydrous conditions. Adequate concentrations of I and II (>1 mM) are easily achieved for electrochemistry and spectroscopy in aqueous solutions.

Cyclic Voltammetry and Spectroelectrochemistry of Electrode-Confined (BV-Q-BV⁶⁺)_n: pH-Dependent Rectification. The most interesting results from studies of I concern the pH-dependent chemistry. We recently published cyclic voltammetry for electrode-confined (BV-Q-BV⁶⁺)_n at low coverage, <10⁻⁹ mol/cm².¹ At high coverage, >10⁻⁸ mol/cm², the essential result from the pH dependence is the same as at low coverage. At high pH the 4ne⁻/2nH⁺ reduction is reversible, (1), whereas at low pH the 4ne⁻/2nH⁺ reduction occurs, but only the 2ne⁻ associated with the reduced viologen centers can be electrochemically withdrawn, (2). At low pH the quinone centers remain reduced, in the QH₂ state, even when scanning to 0.5 V vs SCE, significantly positive of the formal potential of the Q/QH₂ for the range of pH 1–9. Thus, the pH-dependent rectification illustrated in Scheme I is apparent for a wide range of coverages of (BV-Q-BV⁶⁺)_n.

The electrochemical response for (BV-Q-BV⁶⁺)_n at high coverage does differ from the low-coverage results (Figure 1). The high-coverage polymer does not exhibit a well-resolved cyclic voltammetry wave that can be attributed to the Q ⇌ QH₂ interconversion that is observed at low coverage at pH ≈ 7. However, the return sweep (from –0.7 to 0.0 V vs SCE) in the high-coverage case at pH ≈ 7 does show an anodic peak, at low sweep rates, that can be attributed to the QH₂ → Q process. At pH ≈ 7 the low-coverage case shows a cyclic voltammogram that is consistent with a simple admixture of the expected electrochemical response for a 2/1 BV²⁺/Q ratio. From Figure 1 it is apparent that the

TABLE I: UV-Vis Absorption Data for Relevant Compounds

species	concn, ×10 ⁵ M ^a	absorpn max, nm (ε, M ⁻¹ cm ⁻¹)
Q (from VI)	100	550 (290) ^b
	1	356 (28 000) ^c
QH ₂ (from VI) ^d	10	320 (5 100)
BV ²⁺ (from IV)	10	260 (22 000)
	1	261 (26 000)
	0.5	260 (26 000)
BV ⁺ (from IV) ^e	10	550 (10 000) ^b
	1	601 (13 000) ^b
	0.5	602 (14 000) ^b
BV ²⁺ -Q-BV ²⁺ (from II)	0.76 ^f	260 (62 000); 356 (28 000) ^c
2BV ²⁺ + Q (from IV + VI)	1.52 ± 0.76	258 (58 000); 356 (27 000) ^c
BV ⁺ -QH ₂ -BV ⁺ (from II) ^e	0.76	534 (42 000) ^b
2BV ⁺ + QH ₂ (from IV + VI) ^e	1.52 ± 0.76	601 (50 000) ^b
BV ⁺ -QH ₂ -BV ⁺ (from II) ^e	0.84 ^f	530 (42 000) ^b
	0.08	535 (34 000) ^b
	0.04	~538 ^{b,g}

^a in pH 7.2 Tris buffer/0.1 M KCl. ^b Only visible absorption listed. ^c Visible absorption not listed. ^d Produced by bulk electrolysis of Q from VI. ^e Produced by adding excess Na₂S₂O₄ to a solution of the oxidized species. ^f Concentration determined from the absorbance of the 356-nm Q peak with ε = 27 800 M⁻¹ cm⁻¹. ^g Absorbance too weak to give accurate value for ε.

low-coverage case shows well-resolved cyclic voltammetry waves, even at fairly high sweep rates. The higher coverage case shows a sweep rate dependence that clearly indicates slow charge transport, because the peak current (at any pH) does not increase linearly with sweep rate at the rates shown. The nonlinear dependence of peak current on the sweep rates sets in at only very modest sweep rates, compared to the response of (BV²⁺)_n (from III) under the same conditions.^{3,4} This result suggests that the diffusion coefficient for charge transport *D*_{CT}, for (BV-Q-BV⁶⁺)_n is smaller than for (BV²⁺)_n, a finding confirmed quantitatively by transient and steady-state measurements described below. The difference in the appearance of the cyclic voltammograms for (BV-Q-BV⁶⁺)_n at low and high coverage can be attributed to the low value of *D*_{CT}.

Considering that the cyclic voltammetry at high coverage does not show a resolved wave for the Q ⇌ QH₂ interconversion, we have undertaken spectroelectrochemical measurements of optically transparent SnO₂ derivatized with a high coverage of (BV-Q-BV⁶⁺)_n to demonstrate, spectroscopically, the pH-dependent rectification. Figure 2 shows the crucial spectroelectrochemical experiment in which cyclic voltammetry at pH 4 indicates that rectification occurs. The (BV-Q-BV⁶⁺)_n state at 0.0 V vs SCE exhibits an absorption at ~350 nm, which is due entirely to Q as deduced from UV-vis spectra of IV and VI in solution. Stepping the potential of the electrode to –0.7 V vs SCE gives a new spectrum which is dominated by the BV⁺ centers, deduced from studies of SnO₂ electrodes modified with III^{3,4} and from spectra of solution BV⁺ species from reduction of IV (Table I). Both the intense 550- and 380-nm absorbances can be entirely attributed to the BV⁺ centers of the 4ne⁻/2nH⁺ reduced (BV-Q-BV⁶⁺)_n, because the reduction of Q centers to give QH₂ results in bleaching of the 350-nm absorbance, from studies of the reduction of VI in solution. Upon stepping the potential of the SnO₂/(BV-QH₂-BV⁴⁺)_n back to 0.0 V vs SCE, the optical spectral changes reveal that the QH₂ centers remain reduced for a long period of time: all of the near-UV and Vis absorption is bleached and, in particular, there is negligible absorbance at 350 nm, characteristic of the oxidized quinone centers. The point is that the BV⁺ absorptions at 380 and 550 nm are rapidly bleached, consistent with oxidation of the BV⁺ centers back to BV²⁺ as deduced from cyclic voltammetry, whereas the 350-nm absorption does not appear on the same time scale. Indeed, the inset in Figure 2 shows the recovery of the 350-nm absorption to take >20 min. Thus, upon holding the electrode at 0.0 V vs SCE, ~0.2 V more positive than E^{o'}(Q/QH₂), the oxidation of QH₂ back to Q is slow.

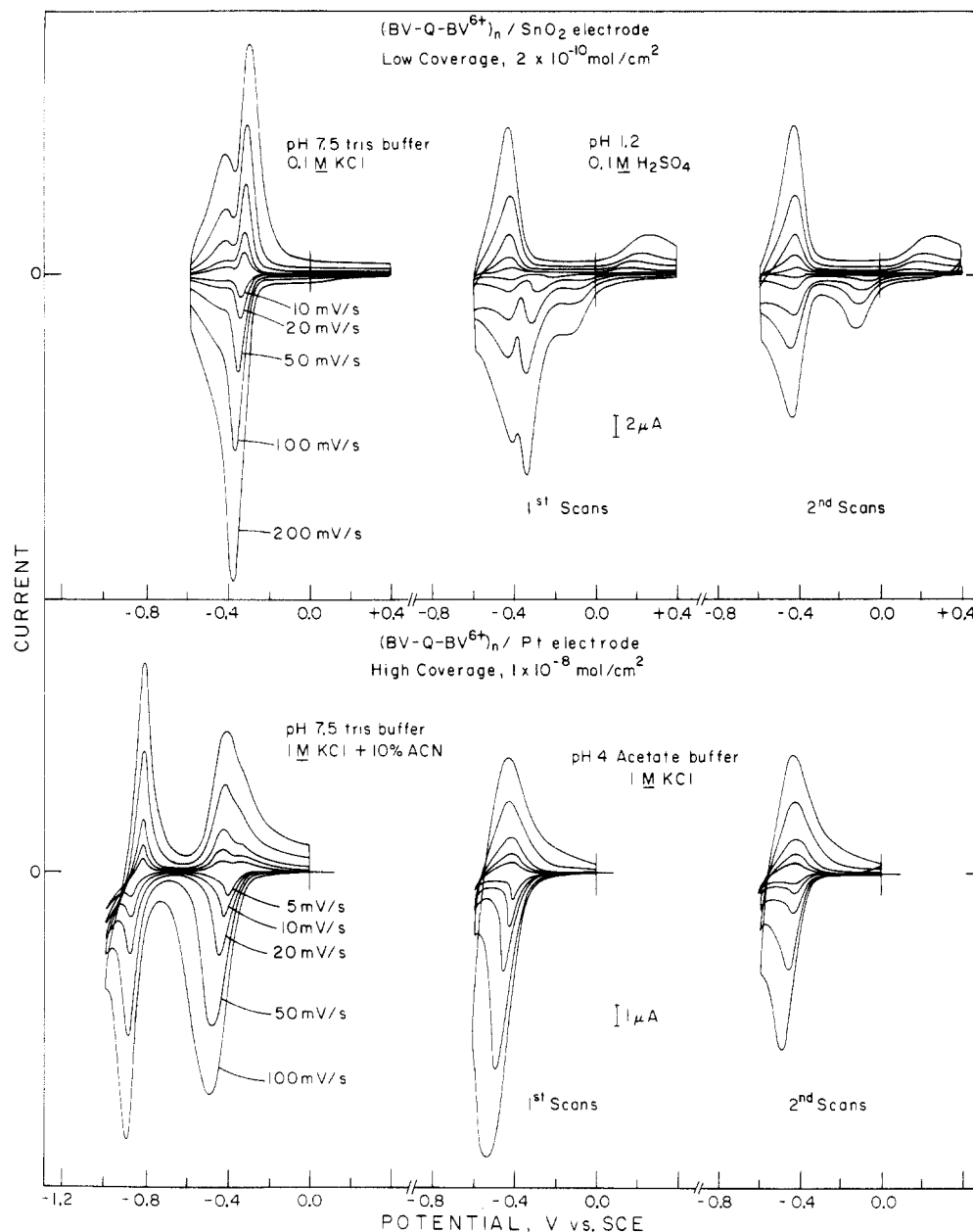


Figure 1. Cyclic voltammetry as a function of sweep rate for a Pt/(BV-Q-BV⁶⁺)_n electrode at high coverage ($\sim 1 \times 10^{-8}$ mol/cm²) and a SnO₂/(BV-Q-BV⁶⁺)_n electrode at low coverage ($\sim 2 \times 10^{-10}$ mol/cm²) for pH 7.5 (no rectification), where first and all succeeding scans are the same, and low pH (rectification), where the first and second scans differ by the amount of charge trapped as QH₂. The second and all succeeding scans are the same at low pH until QH₂ is reoxidized to Q.

In fact, the recovery of the 350-nm absorption occurs at essentially the same rate when the electrode is removed from potential control. Presumably, O₂ (or some other impurity oxidant) regenerates Q according to (3), consistent with the fact that O₂ reacts with QH₂ from VI to give Q and H₂O₂.¹⁷ In contrast to the low-pH spectroelectrochemistry of SnO₂/(BV-QH₂-BV⁶⁺)_n, where rectification is found, spectroelectrochemical measurements at pH 7 show reversible optical spectral changes consistent with a reversible $4ne^-/2nH^+$ reduction represented by (1). Thus, optical spectral changes accompanying potential variation of SnO₂/(BV-Q-BV⁶⁺)_n electrodes provide molecular specific evidence for charge trapping at low pH in the form of QH₂ centers in the polymer.

The essence of the results conveyed in Figures 1 and 2 have been reproduced for a wide range of electrolyte types of concentrations. In addition the pH variation has been achieved with a variety of buffer systems, to ensure that the effects are due to variation in pH and not due to variation in the nature of other

materials in the solution. While there are some minor changes in electrochemical behavior with variation in the aqueous medium, the essential finding is that pH-dependent rectification occurs as represented in Scheme I.

The cyclic voltammetry of (BV-Q-BV⁶⁺)_n reveals several additional features. The $6ne^-/2nH^+$ reduction can be effected by moving the potential more negative than the potential associated with $E^{\circ'}(BV^{+/0}) \approx -0.9$ V vs SCE (Figure 1). The second reduction wave associated with the BV^{+/0} system is well-resolved for low and high coverages of (BV-Q-BV⁶⁺)_n at pH's where H₂ evolution does not obscure the electrochemical response of the polymer. Generally, SnO₂, rather than Pt, is the electrode of choice for observing the wave for the BV^{+/0} system, because the H₂ evolution overvoltage is large on SnO₂. Often, the addition of CH₃CN (to 10% by volume) to the aqueous solution is useful in more effectively suppressing H₂ evolution. The wave attributable to the BV^{+/0} system is unexceptional in that it appears at a potential and with an area consistent with the formulation of the molecule. The BV⁰ state is not as durable as the BV⁺ or BV²⁺ states in aqueous solution, and as a consequence, we have not focused effort on the properties of the BV⁰ centers.

(17) (a) Tender, L. M.; Smith, D. K.; Lane, G. A.; Wrighton, M. S., to be submitted. (b) Calabrese, G. C.; Buchanan, R. M.; Wrighton, M. S. *J. Am. Chem. Soc.* **1983**, *105*, 5594.

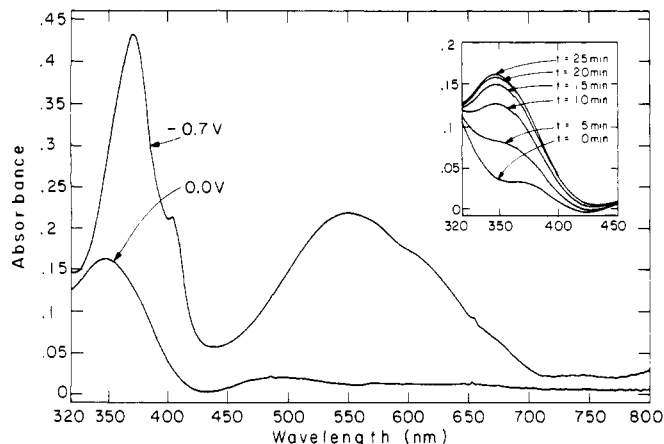


Figure 2. Transmission spectrum of a $\text{SnO}_2/(\text{BV-Q-BV}^{6+})_n$ electrode in 1.0 M LiCl, pH 4 at 0.0 V vs SCE, where the polymer is in the $(\text{BV-Q-BV}^{6+})_n$ state, and then at -0.7 V vs SCE, where the polymer is in the $(\text{BV-QH}_2\text{-BV}^{4+})_n$ state. Upon switching the potential back to 0.0 V vs SCE, the visible absorbance (~ 550 nm) decays immediately to the initial value and the 320–450-nm region goes immediately to the curve marked “ $t = 0$ min” in the inset, consistent with formation of the $(\text{BV-QH}_2\text{-BV}^{6+})_n$ state of the polymer where the viologen units are fully oxidized and the quinone unit remains reduced, despite the fact that $E^0(\text{Q}/\text{QH}_2)$ is more negative than 0.0 V vs SCE. The inset shows the growth of 350-nm absorbance in time associated with the $(\text{BV-QH}_2\text{-BV}^{6+})_n \rightarrow (\text{BV-Q-BV}^{6+})_n$ conversion.

Another feature of relevance in the cyclic voltammogram of $(\text{BV-Q-BV}^{6+})_n$ is that at low pH, where rectification is observed, there is generally a small wave relative to the $\text{BV}^{2+}/\text{BV}^{+}$ wave that can be attributed to the direct interconversion of the Q/QH_2 system. This wave is clearly observable in the cyclic voltammograms in Figure 1 of the low-coverage electrode at pH 1.2. Both first and second scans at each sweep rate show a quasi-reversible wave centered at $+0.05$ V vs SCE. This wave is essentially the same as that observed with $(\text{Q})_n$ derivatized (from V) electrodes in pH 1.2 solution (Figure 3). Similar small waves are observed at the reversible potential for quinone reduction in other acidic media as well. The small wave is also present at high ($>10^{-8}$

mol/cm^2) coverages, although in such cases it is not observable on the same sensitivity scale used to monitor the $\text{BV}^{2+} \rightleftharpoons \text{BV}^+$ interconversion. The area of the wave is apparently independent of coverage down to a total coverage of 1×10^{-10} mol/cm^2 of $(\text{BV-Q-BV}^{6+})_n$ and is consistent with $\sim 4 \times 10^{-11}$ mol/cm^2 of $\text{Q} \rightleftharpoons \text{QH}_2$ interconversion. This result is consistent with the conclusion that a fraction of the molecules of I bind to the electrode surface in a manner that permits direct equilibration of the electrode with the Q/QH_2 center of the $(\text{BV-Q-BV}^{6+})_n$ system. However, at any coverage of $(\text{BV-Q-BV}^{6+})_n$ investigated there appears to be a degree of rectification; that is, even at 1×10^{-10} mol/cm^2 the majority of Q centers are only reducible to QH_2 upon scanning more negative than the thermodynamically required potential, a potential close to the onset of BV^{2+} reduction of BV^+ , and the QH_2 thus formed is not oxidizable even when the electrode potential is moved more positive than that of the small wave for the Q/QH_2 in direct equilibrium with the electrode. The main point is that there is a small fraction of the innermost Q centers that can undergo more or less reversible electrochemical reduction. This is not a surprising finding, considering that the linkages between the BV^{2+} and Q centers are flexible. It is obvious that the fact that the $-\text{Si}(\text{OMe})_3$ groups are on the BV^{2+} centers does not ensure that the Q centers will be held far away from the electrode surface, and there are many possible conformations of a BV-Q-BV^{6+} unit bound to a surface.

The final issue of significance in connection with the cyclic voltammetry of electrode-confined $(\text{BV-Q-BV}^{6+})_n$ concerns the consequences of positive potential excursions. Except for Q/QH_2 centers directly accessible, potential excursions to $+0.2$ V vs SCE yield no electrochemical response independent of pH (1–9), of coverage, or of whether the scan sequence begins at 0.0 V vs SCE and goes negative and then to $+0.2$ V vs SCE. The point is a positive excursion to $+0.2$ V vs SCE does not oxidize “trapped” QH_2 centers. More positive potential excursions than $+0.2$ V vs SCE can have an effect on the behavior of the $(\text{BV-Q-BV}^{6+})_n$ system. At potentials positive of $\sim +0.6$ V vs SCE there is irreversible oxidative degradation. The nature of the oxidation chemistry is not known, but there is the possibility of oxidation at the $-\text{NH}-$ attached to the quinone ring. Potential excursions beyond $+0.2$ V vs SCE (starting at 0.0 V vs SCE and initially scanning positive) irreproducibly reveal a redox system in the

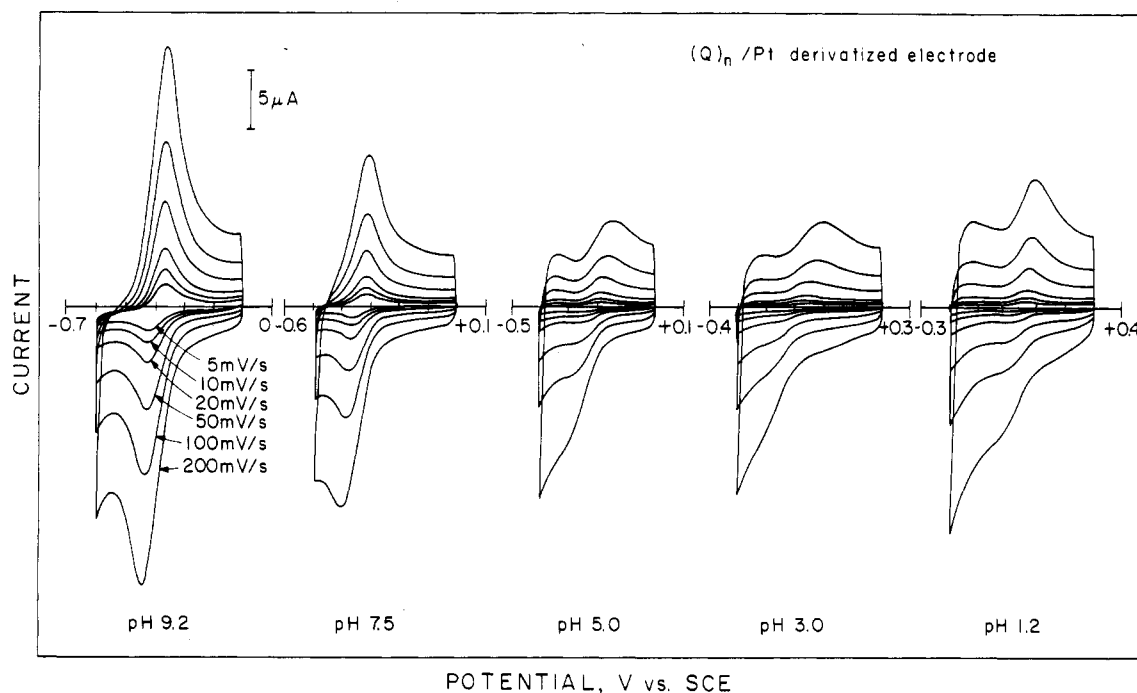


Figure 3. Cyclic voltammetry of Pt electrodes modified with (Q/QH_2) (from V) as a function of pH and sweep rate to establish the dependence of $E^0(\text{Q}/\text{QH}_2)$ on pH under the same conditions as for $(\text{BV-Q-BV}^{6+})_n$ in Figures 1 and 2. Note that the apparent electrochemical coverage at 10 mV/s ranges from $\sim 9 \times 10^{-10}$ mol/cm^2 at pH 9 to $\sim 8 \times 10^{-11}$ mol/cm^2 at pH 1.2. Electrostatic binding of $\text{Fe}(\text{CN})_6^{3-/4-}$ into the polycationic $(\text{Q})_n$ (from V) shows a coverage of at least 3×10^{-9} mol/cm^2 .

TABLE II: $E^{\circ'}$ Values at 298 K of $BV^{2+/+}$ and Q/QH_2 from Various Molecules^a

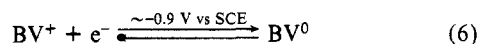
medium	$BV^{2+/+}$			
	solution		surface-confined	
	$BV^{2+/+}$ (from IV), V vs SCE	$BV-Q-BV^{6+}$ (from II), V vs SCE	$(BV^{2+/+})_n$ (from III), V vs SCE	$(BV-Q-BV^{6+})_n$ (from I), V vs SCE
pH 9.2	-0.56	~-0.5 ^b	-0.49	-0.40 to -0.43
pH 7.5	-0.57	~-0.5 ^b	-0.49	-0.40 to -0.43
pH 5.0	-0.57	~-0.5 ^b	-0.49	-0.40 to -0.43
pH 3.0	~-0.5 ^b	~-0.5 ^b	-0.44	-0.40 to -0.43
pH 1.2	-0.58	~-0.5 ^b	-0.47	-0.43

medium	Q/QH_2			
	solution		surface-confined	
	Q (from VI), V vs SCE	$BV-Q-BV^{6+}$ (from II), V vs SCE	$(Q)_n$ (from V), V vs SCE	$(BV-Q-BV^{6+})_n$ (from I), V vs SCE
pH 9.2	-0.36	-0.35	-0.40	-0.38
pH 7.5	-0.31	-0.31	-0.33	-0.32
pH 5.0	-0.18	-0.18 ^c	-0.21	-0.17 ^c
pH 3.0	-0.07	-0.09 ^c	-0.10	-0.10 ^c
pH 1.2	+0.05	+0.04 ^c	+0.04	+0.05 ^c

^a All values shown were determined by cyclic voltammetry. $E^{\circ'}$ is taken to be the average position of the anodic and cathodic current peaks. The base electrolyte was 0.1 M KCl except at pH 1.2 where 0.1 M H_2SO_4 was used. For species in solution the concentration was ~ 1 mM and surface-confined measurements were made at coverages of $\sim 10^{-10}$ mol/cm². ^b $BV^{2+/+}$ wave was distorted due to precipitation onto the electrode surface. ^c $E^{\circ'}$ of small surface-confined Q wave. See text for explanation.

vicinity of +0.3 V vs SCE. The wave is typically broad and of low integrated area (<5%) compared to the $BV^{2+/+}$ wave of $(BV-Q-BV^{6+})_n$. However, the release of trapped charge from QH_2 can be catalyzed by the redox system at $\sim +0.3$ V vs SCE. This redox system, apparently an impurity of unknown origin, can be eliminated by cleaning the glassware carefully, isolating the counter electrode in a separate compartment, and using only very pure H_2SO_4 as the electrolyte. Figure 1 shows that if these precautions are used, along with thorough deoxygenation, even a low-coverage electrode can be scanned out to +0.4 V vs SCE at 10 mV/s without any reoxidation of the trapped QH_2 to Q. A thorough study of the chemically catalyzed release of trapped charge (change in pH, solution redox mediators) is in progress and will be reported elsewhere.^{17a}

Cyclic Voltammetry of Components of $(BV-Q-BV^{6+})_n$ and of II. The electrochemistry of BV^{2+} subunits of $(BV-Q-BV^{6+})_n$ (from III) has been well-characterized by studies of IV in solution and by studies of $(BV^{2+})_n$ on electrode surfaces.^{3,4} The BV^{2+} subunits are pH-insensitive, one-electron redox systems. Equations 5 and 6 describe the electrochemistry of $BV^{2+/+}$ system in solution from



IV or as a polymer $(BV^{2+/+})_n$. $E^{\circ'}$ values for the first viologen reduction in solution, in $(BV^{2+/+})_n$ and in $(BV-Q-BV^{6+})_n$ are listed in Table II. The value of $E^{\circ'}$ is taken to be the average position of the anodic and cathodic current peak in a cyclic voltammetry scan. As expected, pH has no effect on the $E^{\circ'}$ of the $BV^{2+/+}$ couple, but there are significant differences among the different forms of viologen. Note especially that $E^{\circ'}$ of BV^{2+} in $(BV-Q-BV^{6+})_n$ is significantly positive of both BV^{2+} in solution and in the homopolymer, $(BV^{2+})_n$.

The electrochemistry of quinone VI has been studied in aqueous solution. Below pH 9 VI undergoes a $2e^-/2H^+$ reduction as represented by eq 7. $E^{\circ'}$ values for the Q/QH_2 couple in solution,



in the homopolymer, $(Q)_n$ (from V), and in $(BV-Q-BV^{6+})_n$ are

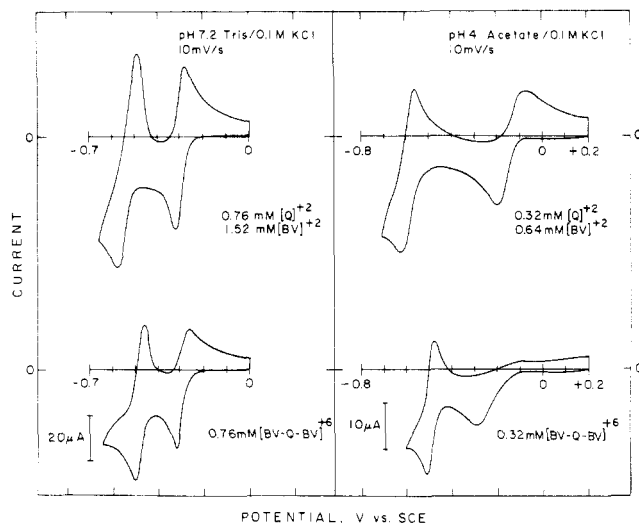


Figure 4. Comparison of the cyclic voltammetry of a solution of II and a solution of 2 to 1 IV and VI at similar concentrations in pH 7.2 and pH 4.

listed in Table II. Unlike BV^{2+} , there is little difference in $E^{\circ'}$ among the different forms of the quinone at a given pH, but there are significant differences in $E^{\circ'}$ at the different pH's. $E^{\circ'}$ values of $(Q)_n$ derivatized electrodes, measured in a variety of buffer systems and electrolyte concentrations, show a 50 ± 5 mV change in $E^{\circ'}$ per pH unit from pH 9 to pH 3. The observed value of $E^{\circ'}$ at pH 1.2, +0.04 V vs SCE, falls slightly above the line established from data for pH 9 to pH 3, possibly indicating additional protonation at this pH.

Representative cyclic voltammograms of $(Q)_n$ derivatized electrodes in different pH's are shown in Figure 3. These reveal an important fact relating to the electrochemistry of the quinone system: charge transport for the Q/QH_2 system is sluggish at best, in comparison to the $(BV^{2+/+})_n$ system, but becomes significantly slower at lower pH's. At relatively low apparent coverages of $(Q/QH_2)_n$, compared to $(BV^{2+/+})_n$, and at any pH, the linear increase of peak current with sweep rate is lost at low sweep rates. The nonlinear increase of peak current at the low sweep rates shows that charge transport is slow. Additionally, note that the apparent electrochemical coverage declines as the pH is lowered. In fact, in such experiments there is not actual loss of electroactive material, because reexamination of the electrochemical response first at pH 9, then at pH 1 (where the apparent coverage is less), and again at pH 9 shows that the exposure and electrochemistry at low pH does not affect the integral of the cyclic voltammetry wave measured at pH 9. Similar results for electrodes modified with an anthraquinone-containing redox polymer have been reported by Degrand and Miller.¹⁸

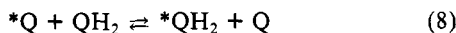
The cyclic voltammograms in Figure 3 suggest that not all of the Q present is electrochemically accessible especially at low pH, but also possibly at pH 9. An alternative method to determine the amount of Q present is to exchange an electroactive anion into the polymer. Recall that each Q unit has a fixed +2 charge; cf. V and VI. Many workers have shown that polycationic polymers strongly bind large inorganic anions such as $Fe(CN)_6^{3-/4-}$.¹⁹ For example, with $(BV^{2+})_n$,^{3a} and a similar alkylviologen polymer,^{19d} a few μM of $Fe(CN)_6^{3-/4-}$ in solution will completely displace the halide counterions in the polymers. In these cases, the amount of bound $Fe(CN)_6^{3-/4-}$, determined by integrating the area of the

(18) Degrand, C.; Miller, L. L. *J. Electroanal. Chem.* **1981**, *117*, 267; *J. Electroanal. Chem.* **1982**, *132*, 163.

(19) (a) Oyama, N.; Anson, F. C. *J. Electrochem. Soc.* **1980**, *127*, 247. (b) Oyama, N.; Shimomura, T.; Shigehara, K.; Anson, F. C. *J. Electroanal. Chem.* **1980**, *112*, 171. (c) Deleted in proof. (d) Bruce, J. A.; Wrighton, M. S. *J. Am. Chem. Soc.* **1982**, *104*, 74. (e) Kuo, K.; Murray, R. W. *J. Electroanal. Chem.* **1982**, *131*, 74. (f) Mortimer, R. J.; Anson, F. C. *J. Electroanal. Chem.* **1982**, *137*, 149. (g) Montgomery, D. D.; Shigehara, K.; Tsuchida, E.; Anson, F. C. *J. Am. Chem. Soc.* **1984**, *106*, 7991. (h) Sumi, K.; Anson, F. C. *J. Phys. Chem.* **1986**, *90*, 3845.

$\text{Fe}(\text{CN})_6^{3-/4-}$ cyclic voltammetry wave, agrees with the coverage expected as determined by integrating the area of the $(\text{BV}^{2+/+})_n$ wave assuming precise charge compensation of the polycationic polymer by $\text{Fe}(\text{CN})_6^{3-/4-}$. However, we find in similar experiments with $(\text{Q})_n$ derivatized electrodes that the area of the $\text{Fe}(\text{CN})_6^{3-/4-}$ wave often indicates that much more polymer is present than the area of the Q/QH_2 wave suggests. With the particular electrode shown in Figure 4 the area of the Q/QH_2 wave at 10 mV/s in pH 7.5 solution corresponds to a coverage of 3×10^{-10} mol/cm², which is typical for $(\text{Q})_n$ electrodes derivatized with V. However, exchanging in $\text{Fe}(\text{CN})_6^{3-/4-}$ shows that the actual amount of polymer present in the Figure 3 electrode is at least 10 times this value. In other cases the coverage obtained by integrating the charge associated with the electrostatically bound $\text{Fe}(\text{CN})_6^{3-/4-}$ is at least 50 times greater than that indicated by the Q/QH_2 wave.

The electrochemical inaccessibility of all of the $(\text{Q}/\text{QH}_2)_n$ shows that the self-exchange process, (8), for the $(\text{Q}/\text{QH}_2)_n$ polymer

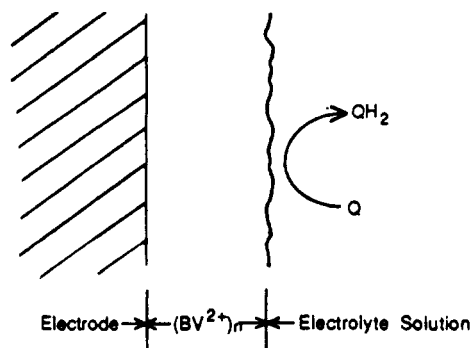


is inadequate to yield complete reduction/oxidation of the Q/QH_2 centers on the time scale of a cyclic voltammogram at 5 mV/s. In terms of the relevance to the pH-dependent rectification associated with $(\text{BV-Q-BV}^{6+})_n$, the important result from $(\text{Q}/\text{QH}_2)_n$ is that the reduction/oxidation via the process represented by (8) is likely too slow to account for the reduction of Q centers in $(\text{BV-Q-BV}^{6+})_n$ at high coverage, particularly at low pH.

The electrochemical response of aqueous solutions containing a 2/1 ratio of IV to VI has been compared to the electrochemical response of II in solution (Figure 4). The mixture of IV and VI gives electrochemistry that is expected on the basis of adding the responses from IV and VI determined independently, at any pH in the range 1–9. Figure 4 includes data for pH 4 and 7 showing that the solution Q/QH_2 system, VI, is pH-dependent and the $\text{BV}^{2+/+}$ system, IV, is insensitive to pH. The cyclic voltammetry wave for the $\text{BV}^{2+/+}$ is somewhat distorted because of the tendency for the BV^+ material to precipitate onto the electrode. However, the cyclic voltammogram of a 2/1 ratio of IV to VI in solution at pH 4 and 7 is essentially the sum of the cyclic voltammograms of IV and VI separately determined. At pH 7 the cyclic voltammogram for II in solution is again, more or less, that expected for a 2/1 ratio of BV^{2+}/Q units. The wave for Q/QH_2 in II is at nearly the same position as the wave for VI, while the $\text{BV}^{2+/+}$ wave in II is slightly more positive than the wave for IV. In contrast, the cyclic voltammogram for II at pH 4 shows unusual behavior: while the $\text{BV}^{2+/+}$ wave is essentially the same as at pH 7, the Q/QH_2 electrochemistry appears to be qualitatively less ideal than at pH 7. The Q to QH_2 reduction process in II occurs with better facility than the oxidation of QH_2 back to Q . In fact, at the sweep rate illustrated in Figure 4 for II at pH 4 the reduction of Q to QH_2 is effectively irreversible. Thus, the solution electrochemistry of II resembles that of electrode-confined $(\text{BV-Q-BV}^{6+})_n$ from I. The rectification illustrated at pH 4 for II, in fact, appears to be due to the fact that a small amount of II adsorbs on the electrode and the $\text{BV}^{2+/+}$ centers are required to "mediate" the reduction of the Q centers of molecules in solution. The peak cathodic current for the $\text{Q} \rightarrow \text{QH}_2$ process in II does occur at a potential more negative than for the $\text{Q} \rightarrow \text{QH}_2$ process of VI, consistent with a mediated redox process. The adsorbed material from II thus behaves in a manner similar to the material from I. Direct evidence for persistent adsorption of II comes from the observation that an electrochemical response like that from electrodes modified with I can be seen first by dipping the Pt electrode into a solution of II followed by examining in solution containing no added II. The response gradually declines during a several-minute period.

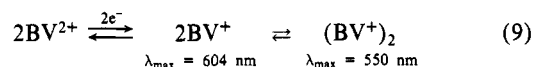
The main conclusion from the study of solution IV and VI is that the electrochemistry $(\text{BV-Q-BV}^{6+})_n$ is not a simple sum of the response of BV^{2+} and Q centers. Study of II shows results similar to those found with $(\text{BV-Q-BV}^{6+})_n$ from I, because II persistently adsorbs on the electrode. Results of the electrochemistry of $(\text{Q}/\text{QH}_2)_n$ from V show that charge transport via the Q/QH_2 centers is poor at any pH and especially so at low pH.

SCHEME III: Arrangement of Electrode Modified with III for the Mediated Reduction of Q (VI) in Solution



The important conclusion is that charge transport via Q/QH_2 exchange in $(\text{BV-Q-BV}^{6+})_n$ is too slow to account for complete reduction of the Q centers.

UV-Vis Spectroscopy of $(\text{BV-Q-BV}^{6+})_n$ and Its Components. Table I summarizes UV-Vis spectroscopy of materials relevant to the behavior of $(\text{BV-Q-BV}^{6+})_n$. As discussed above in connection with the pH-dependent rectification, the optical spectroelectrochemistry of $\text{SnO}_2/(\text{BV-Q-BV}^{6+})_n$ Figure 2, is consistent with the spectral changes associated with electrochemistry of the $\text{BV}^{2+/+}$ and Q/QH_2 subunits. An issue of concern is whether the BV^{2+} subunits of I and II interact with each other. It is known that BV^+ centers reversibly aggregate, (9),²⁰ and there is an



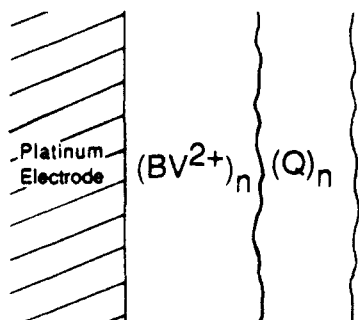
associated optical spectral change. Data in Table I show that below $\sim 10^{-4}$ M the absorption maximum upon one-electron reduction of IV is at 604 nm, characteristic of BV^+ , whereas at higher concentrations the absorption blue shifts to ~ 555 nm, characteristic of the dimer, $(\text{BV}^+)_2$. The $\text{SnO}_2/(\text{BV-Q-BV}^{6+})_n$ shows a visible absorption of ~ 550 nm upon reduction of BV^{2+} centers by one electron. The position of the absorption maximum is consistent with interaction of BV^+ centers in the polymer. The spectroelectrochemistry of II in solution shows that reduction of the BV^{2+} centers gives an intense visible absorption at ~ 530 nm. Although the visible absorption maximum shifts to the red slightly upon dilution, even at 4×10^{-7} M the visible absorption maximum associated with the BV^+ centers in II is at ~ 538 nm and not at 604 nm. While aggregation of reduced II might be expected to occur at lower concentration than reduced IV, because the solubility of II is low, the inability to see the red-shifted visible absorption suggests that the $\text{BV}^{2+/+}$ centers of II (and presumably I) can interact *intramolecularly*. The spectral results thus favor conformations of I and II that allow intramolecular BV^+-BV^+ interaction.

Redox Reaction between the Q/QH_2 and $\text{BV}^{2+/+}$ Systems and Behavior of $(\text{BV}^{2+/+})_n/(\text{Q}/\text{QH}_2)$ Bilayers. The facts that (i) the $(\text{Q})_n$ polymers are not rapidly (or at low pH's completely) reducible and (ii) electrode-confined $(\text{BV-Q-BV}^{6+})_n$ shows pH-dependent rectification are consistent with the conclusion that the reduction of Q in $(\text{BV-Q-BV}^{6+})_n$ polymer occurs via the process represented by (4). Several experiments have been carried out to establish that redox chemistry can occur according to (4) and with a rate that is fast.

Rotating disks modified with $(\text{BV}^{2+})_n$ from III can be used to reduce VI in solution. Presumably due to the fact that the $(\text{BV}^{2+/+})_n$ system and VI are positively charged, there is no evidence for penetration of VI through the $(\text{BV}^{2+/+})_n$ film. That is, the reduction of VI is not observed at the expected $E^{\circ'}$ for electrodes modified with III. Rather, the $(\text{BV}^{2+/+})_n$ system mediates reduction of VI and the onset of current corresponds

(20) (a) Kosower, E. M.; Cotter, J. L. *J. Am. Chem. Soc.* **1964**, *86*, 5524. (b) Evans, A. G.; Evans, J. C.; Baker, M. W. *J. Chem. Soc., Perkin Trans. 2* **1977**, 1787. (c) Furue, M.; Nozakura, S. *Chem. Lett.* **1980**, 821. (d) Deronzier, A.; Galland, B.; Vieira, M. *Nouv. J. Chim.* **1982**, *6*, 97.

SCHEME IV: Bilayer Assembly from First Modifying an Electrode with III Followed by Modification with V (The System Shows pH-Dependent Rectification; Figure 5)

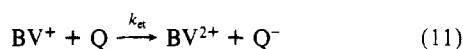


to the onset of reduction of the surface-confined BV^{2+} . Accordingly, the reduction of the solution Q centers to QH_2 occurs at the outermost portion of the $(BV^{2+/+})_n$ polymer (Scheme III). Unidirectional charge transfer to a solution of Q is evident from cyclic voltammetry at a nonrotating microdisk electrode modified with $(BV^{2+})_n$. Considerably more charge is passed in the cathodic portion of the cyclic voltammogram than in the anodic portion in solutions containing Q . The reduced QH_2 is not capable of reducing BV^{2+} to BV^+ at pH 5, and this is the rationale for the unidirectional charge transfer observed. At a $(BV^{2+})_n$ coverage of 6×10^{-9} mol/cm² a conventional macroscopic disk (~ 3 -mm diameter) will reduce 1 mM Q at pH 5 to QH_2 at a mass transport limited rate up to a (rotation velocity)^{1/2}, $\omega^{1/2}$, = 32 (10 000 rpm) when the electrode is held at -0.7 V vs SCE where the polymer is in the $(BV^+)_n$ state. The mass transport limited reduction of Q at conventional rotating disks modified with $(BV^{2+})_n$ establishes a reasonably large rate for mediated reduction of Q by BV^+ .

Rotating microdisk electrodes modified with $(BV^{2+})_n$ can be used to achieve higher effective rotation velocities such that kinetic limitations can be investigated.¹⁶ A 25- μ m-diameter microdisk electrode, mounted off-center in a 3-mm-diameter plane and derivatized with $(BV^{2+})_n$ ($\Gamma = 2.1 \times 10^{-8}$ mol/cm²) was studied in a 0.1 M KCl solution buffered to pH 5 with $CH_3COOH/Na[CH_3COO]$ (0.1 M) containing 1 mM Q . Current at high effective rotation rates is limited by the kinetics of charge transfer at the interface, and i_k , the kinetically limited current at infinite rotation rate, may be determined from the intercept of the Koutecky-Levich plot (i^{-1} vs $\omega_{eff}^{-1/2}$); i_k is then related to k_{et} by (10).¹⁶ In (10) n is the number of e^- 's transferred, F is Faraday's

$$i_k = nFAc_Q\Gamma k_{et} \quad (10)$$

constant, A is the electrode area, c_Q is the concentration of Q , and Γ is the coverage of the BV^+ -reducing equivalents in one monolayer (10^{-10} mol/cm²) of the outermost region of the polymer. For the coverage of $(BV^{2+})_n$ used we have determined experimentally that charge transport through the film is not completely limited by the charge-transport properties of the polymer, allowing determination of k_{et} .¹⁶ We assume that k_{et} is associated with a rate-determining one-electron transfer from BV^+ to Q , (11). i_k



is observed to be proportional to Q concentration as is expected for the case of a kinetically limited current. The value of k_{et} was found to be 4×10^5 M⁻¹ s⁻¹, where the effective $\omega^{1/2} = 160$ at 10 000 rpm for the microdisk used.¹⁶ The mediated reduction of solution Q (from VI) at $(BV^{2+})_n$ -coated electrodes thus establishes that the process represented by (4) can occur rapidly at pH's where rectification is observed for $(BV-Q-BV^{6+})_n$ -coated electrodes.

Experimental results described so far show that BV^+ will reduce Q to QH_2 at a reasonably rapid rate. The reverse-reaction, $2e^-$ oxidation of QH_2 by BV^{2+} can also be demonstrated. Voltammetry of a Pt/ $(BV^{2+})_n$ electrode (coverage = 2×10^{-8} mol/cm²) in 1 mM QH_2 at pH 7.5 shows a wave for QH_2 oxidation on the positive side of the $BV^{2+/+}$ wave. Since $E^{0'}$ of Q/QH_2 is -0.49 V vs SCE, this represents a 180-mV uphill reaction. The rate constant for oxidation of QH_2 by $(BV^{2+})_n$ has not been measured,

SCHEME V: Microelectrode Array for Generator/Collector Experiments; cf. Figures 6 and 7

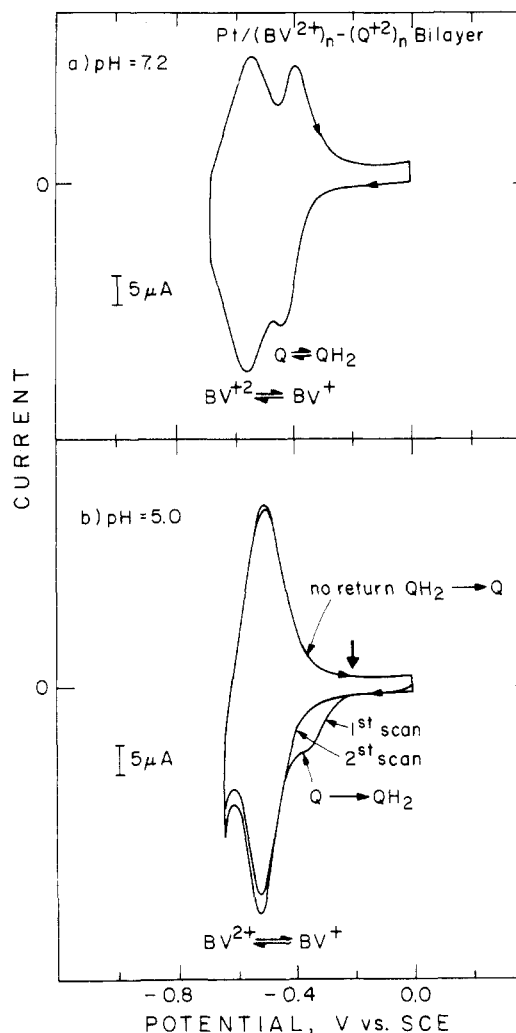
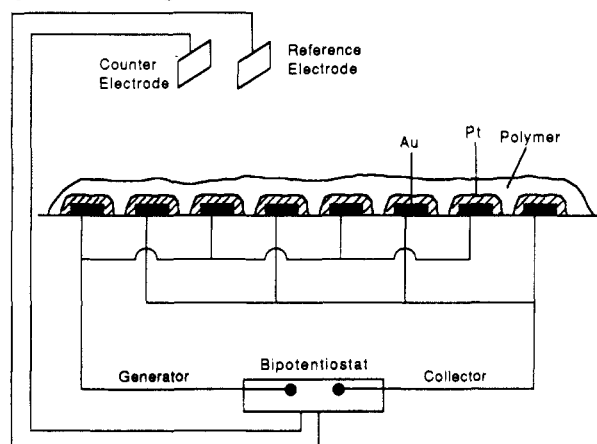


Figure 5. Electrochemical response of bilayer assembly shown in Scheme IV at pH 7.2 (no rectification) and at pH 5 (rectification) at $(BV^{2+/+})_n$ coverage of 6×10^{-9} mol/cm² and $(Q/QH_2)_n$ coverage of 1×10^{-9} mol/cm².

but the steady-state current density observed in a stirred solution exceeds 0.18 mA/cm². Thus, the cross redox reaction represented by (4) can be regarded as a fast equilibrium at pH 7.5.

The final experiments of relevance concerning the redox reaction of $BV^{2+/+}$ with Q/QH_2 concern the demonstration of a "conventional" bilayer that shows pH-dependent rectification.^{6,7} The bilayer assembly represented by Scheme IV has been made by first modifying a Pt electrode with III to give 5×10^{-9} mol/cm² $(BV^{2+/+})_n$. The electrode was then modified with V. The fact

that the positively charged species VI does not penetrate the $(BV^{2+})_n$ ensures the structure represented in Scheme IV. Figure 5 illustrates the electrochemical response of the bilayer at pH 7.2 and at pH 5. At pH 7.2 the bilayer can be completely reduced, because BV^+ is capable of reducing Q to QH_2 , and all of the charge added can be removed because $E^{\circ'}(Q/QH_2)$ and $E^{\circ'}(BV^{2+}/+)$ are sufficiently close that the reverse of (4) can occur. But at pH 5, the reduction of Q to QH_2 is irreversible because the QH_2 is incapable of reducing the BV^{2+} . Unfortunately, the bilayer does not behave ideally, owing to the poor charge transport of the $(Q/QH_2)_n$ layer at low pH. Only a small fraction of the Q accessed at pH 7.2 is in fact reducible at low pH (Figure 5). This is another manifestation of the poor Q/ QH_2 self-exchange process deduced from studies of electrodes modified only with V (vide supra). The behavior of the bilayer assembly $(BV^{2+}/+)_n/(Q/QH_2)_n$ is consistent with the behavior of the $(BV-Q-BV^{6+})_n$ system in that pH-dependent rectification occurs and only the Q centers very close to $BV^{2+}/+$ centers are electrochemically accessible. It is important to underscore the fact that the amount of charge associated with reduction of $(BV-Q-BV^{6+})_n$ is pH-independent and reduction always corresponds to the reduction of all material bound to the surface. Large amounts of Q in $(BV-Q-BV^{6+})_n$ are thus accessible electrochemically via the mediation of reduction of the Q centers by the $BV^{2+}/+$ centers. Thus, the "homogeneous" bilayer system $(BV-Q-BV^{6+})_n$ is capable of storing more charge than the sandwich bilayer in Scheme IV, owing to the fact that all Q centers are accessible in $(BV-Q-BV^{6+})_n$.

Steady-State Charge-Transport Properties of $(BV-Q-BV^{6+})_n$. The charge-transport properties of $(BV-Q-BV^{6+})_n$ have been investigated by steady-state experiments and by potential-step experiments. Derivatized Au microelectrode arrays were used to determine the medium dependence of the steady-state charge transport of $(BV-Q-BV^{6+})_n$. The Au microelectrodes (each initially $\sim 50 \mu\text{m}$ long $\times 2.4 \mu\text{m}$ wide $\times 0.1 \mu\text{m}$ high and separated from each other by $\sim 1.4 \mu\text{m}$ ^{14a}) are first platinized to close the gap between them to as small a value as possible. The microelectrode array is then derivatized with I to "connect" the microelectrodes with $(BV-Q-BV^{6+})_n$. Scheme V illustrates the modified microelectrode array as well as the wiring scheme used in steady-state charge-transport experiments. Figure 6 shows a scanning electron micrograph of a modified microelectrode array showing the average spacing between the platinized microelectrodes to be $\sim 0.3 \mu\text{m}$. The array illustrated in Figure 6 is coated with $(BV-Q-BV^{6+})_n$ at a coverage of $\sim 1.0 \times 10^{-8} \text{ mol/cm}^2$. The polymer appears smooth at the highest resolution used in the microscopy, $\sim 200 \text{ \AA}$.

The steady-state charge-transport properties of the $(BV-Q-BV^{6+})_n$ have been determined by using a microelectrode array like that sketched in Scheme V and shown in Figure 6. The $(BV-Q-BV^{6+})_n$ -modified array is immersed in the desired electrolyte solution and microelectrodes 1, 3, 5, and 7 are used as the "generator" and 2, 4, 6, and 8 are used as the "collector".^{14,21} The collector electrode is held at 0.0 V vs SCE, and the current at the collector and at the generator is monitored upon scanning the potential of the generator from 0.0 V vs SCE to -0.7 V vs SCE . Such experimentation has recently been reported for poly(vinylferrocene)-connected microelectrodes.^{14a} The methodology resembles a ring-disk electrochemical²² experiment where the generator is the disk and the collector is the ring.²¹ In the present case, the generator/collector experiment provides a convenient method for the determination of the differences in steady-state charge-transport properties of $(BV-Q-BV^{6+})_n$ as pH and electrolyte are varied.

Figure 7 illustrates typical data for steady-state charge-transport properties of a $(BV-Q-BV^{6+})_n$ -coated microelectrode array. The full generator/collector current-voltage curves are shown for two pH's, and the figure also shows a plot of the pH dependence of

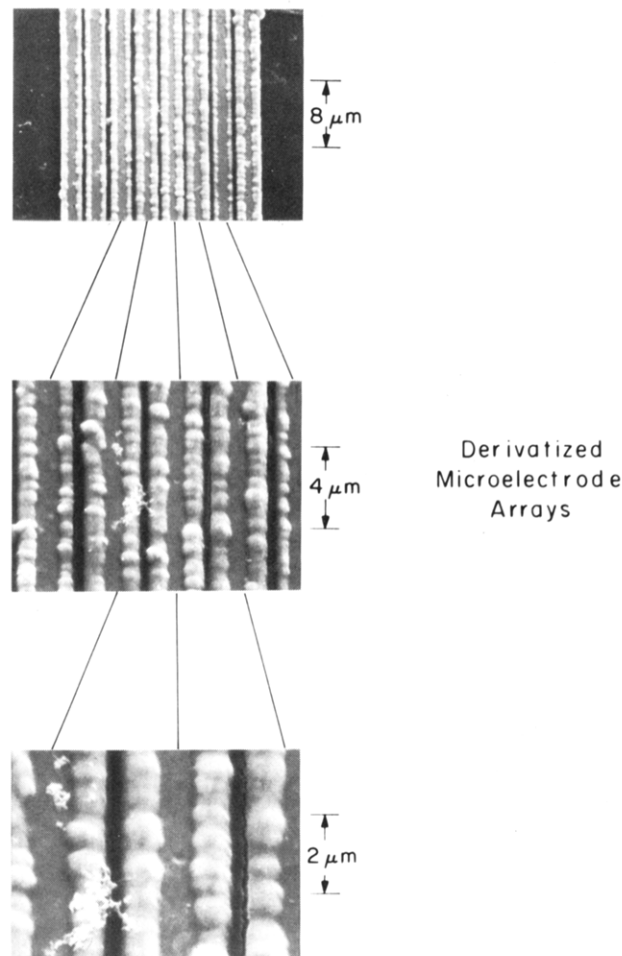


Figure 6. Scanning electron micrograph of a Au microelectrode array first platinized and then derivatized with $(BV-Q-BV^{6+})_n$ at a coverage of $1.0 \times 10^{-8} \text{ mol/cm}^2$ to "connect" each of the microelectrodes with the redox polymer; cf. Scheme V.

the steady-state generator-collector current at a generator potential of -0.7 V vs SCE and a collector potential of 0.0 V vs SCE . The data show that there is steady-state current between the $(BV-Q-BV^{6+})_n$ -connected microelectrodes when the potential of the generator is moved to a potential where the BV^{2+} centers of the polymer begin to be reduced. The steady-state current reaches a plateau when the generator reaches approximately -0.6 V vs SCE where the BV^{2+} centers are fully reduced (to the BV^+ state) and the collector is held at 0.0 V vs SCE . Under such conditions, $[BV^{2+}] \approx 0$ at the generator and $[BV^+] \approx 0$ at the collector, the largest possible concentration gradient exists, giving the plateau in current through the polymer. Essentially the same current-potential relationship holds at all pH's investigated, pH 6–10, but the magnitude of the plateau current depends on pH with the lower pH's giving smaller current. The pH 10 data point also appears to give a lower plateau current, but the data are not as reliable as the pH 6–9 data, because the observed coverage of $(BV-Q-BV^{6+})_n$ declines on the time scale of the experiment. For pH's ≥ 10 the $(BV-Q-BV^{6+})_n$ polymer degrades, presumably due to base-induced hydrolysis of the Si–O–Si linkages.

An actual value of the effective diffusion coefficient for charge transport, D_{CT} , for $(BV-Q-BV^{6+})_n$ requires knowing the nature and concentration of charge-carrying redox centers in the polymer. The nature of the charge-carrying species in $(BV-Q-BV^{6+})_n$ at low pH is logically the $BV^{2+}/+$ system. Charge transport via the Q/ QH_2 system is not reasonable because the $(Q/QH_2)_n$ polymer from V shows poor charge transport, especially at low pH. Accordingly, charge transport at low pH can be regarded as occurring exclusively via the $BV^{2+}/+$ subunits, (5), because the cross redox process involving the Q subunits, (4), is effectively unidirectional at low pH's. The effectively irreversible formation of QH_2 is due

(21) Bard, A. J.; Crayston, J. A.; Kittlesen, G. P.; Shea, T. V.; Wrighton, M. S. *Anal. Chem.* **1986**, *58*, 2321.

(22) Faulkner, L. R.; Bard, A. J. *Electrochemical Methods*; Wiley: New York, 1980; pp 300–304.

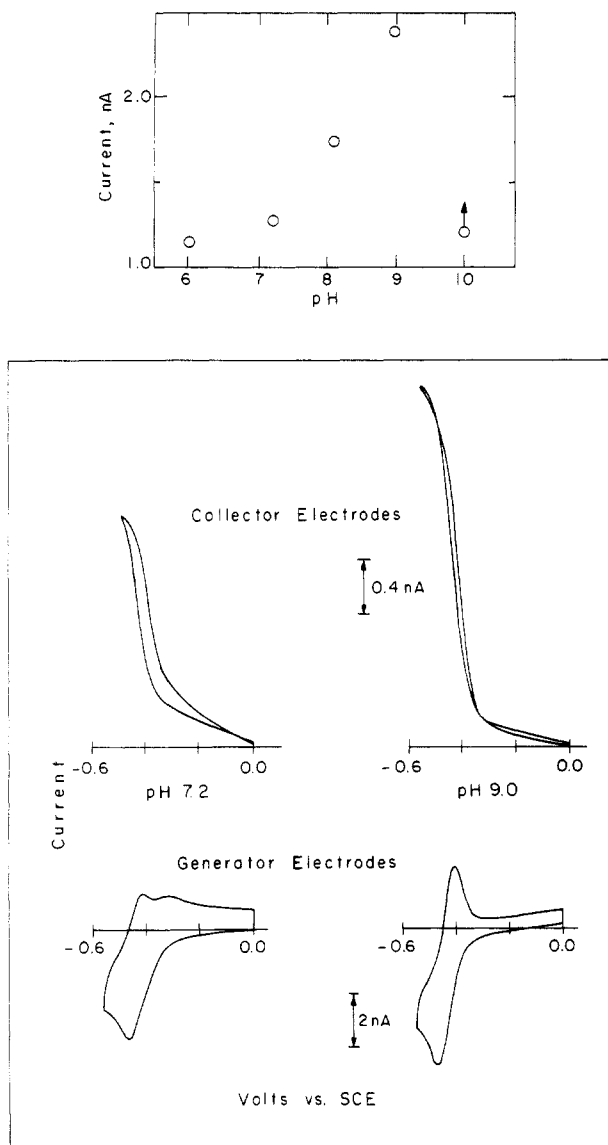


Figure 7. Data showing pH dependence of the steady-state charge-transport rate in $(\text{BV-Q-BV}^{6+})_n$ at 298 K. The top portion shows a summary of the maximum steady-state current passing between the "generator" microelectrodes (1, 3, 5, 7) and the "collector" microelectrodes (2, 4, 6, 8) when the generator is at -0.6 V vs SCE and the collector is at 0.0 V vs SCE. The array used is that shown in Figure 6 and sketched in Scheme V. The bottom current-voltage curves illustrate actual data showing the generator current and collector current vs generator potential for a sweep rate of 10 mV/s at a collector potential of 0.0 V vs SCE. Data are for a 0.5 M sodium tosylate base electrolyte with variation in pH achieved with Tris buffer. The pH 10 point has a large error because the polymer degraded during the experiment owing to base-induced decomposition.

to the fact that QH_2 is thermodynamically incapable of reducing BV^{2+} at low pH's. Thus, at low pH the movement of the generator electrode to -0.7 V vs SCE, while holding the collector at 0.00 V vs SCE, results in the reduction of all Q centers in the polymer (with the exception of the small fraction of Q centers directly accessible to the collector electrode). The steady-state current that results is from the concentration gradient of $\text{BV}^{2+/+}$, $[\text{BV}^{2+}] = 0$ at the generator, and $[\text{BV}^{+}] = 0$ at the collector.

In order to determine concentration of charge-carrying centers in $(\text{BV-Q-BV}^{6+})_n$ the thickness vs coverage was measured (Figure 8). The data in Figure 8 allow a calculation of the concentration of BV-Q-BV^{6+} units as ~ 0.8 M in the dry film. Thus, the concentration of BV^{2+} units is ~ 1.6 M. The concentration of BV^{2+} units in $(\text{BV}^{2+})_n$ from III is ~ 2.2 M under the same conditions.^{3,4} It should be realized that the thickness of the polymer will be larger in electrolyte solution due to solvent swelling, yielding a lower concentration of the subunits of the polymer. Preliminary

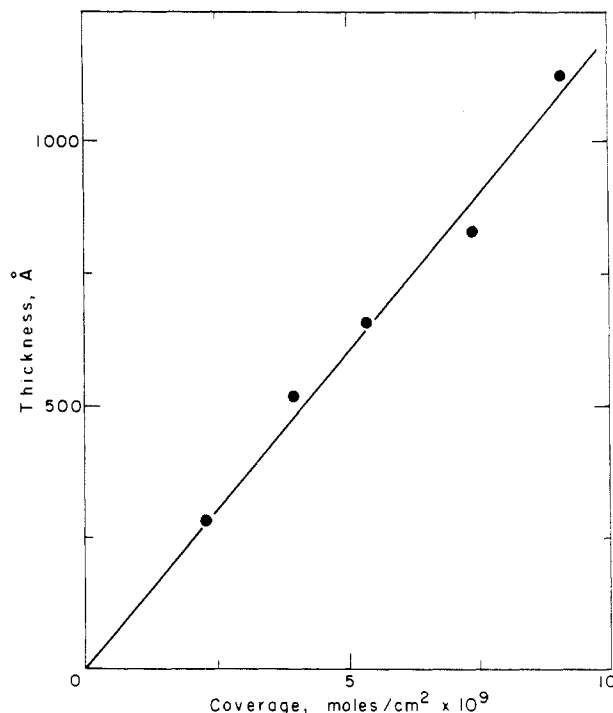


Figure 8. Thickness of a "dry" film of $(\text{BV-Q-BV}^{6+})_n$ charge compensated with Cl^- as a function of electrochemically assayed coverage. The thickness was determined by using a surface profile measuring device; cf. Experimental Section.

measurements indicate that the solvent swelling of $(\text{BV-Q-BV}^{6+})_n$ could be as much as a factor of 2, much larger than for $(\text{BV}^{2+})_n$.^{3b} This may be due to the flexible nature of the monomer unit in $(\text{BV-Q-BV}^{6+})_n$ compared to $(\text{BV}^{2+})_n$. We have also observed that cationic substrates such as $\text{Ru}(\text{NH}_3)_6^{3+}$ freely diffuse through the $(\text{BV-Q-BV}^{6+})_n$ polymer as evidenced by electrochemical measurements at both stationary and rotating electrodes modified with I. At the same coverage of BV^{2+} units, $(\text{BV}^{2+})_n$ from III is blocking to the penetration of $\text{Ru}(\text{NH}_3)_6^{3+}$.³ We believe that the ability of the $(\text{BV-Q-BV}^{6+})_n$ polymer to swell considerably, opening up a large pore structure in the polymer, plays an important role in increasing both cation and anion mobility within the polymer film. The consequence of solvent swelling is that the BV^{2+} concentration for $(\text{BV-Q-BV}^{6+})_n$ in electrolyte solution may be as low as 0.8 M.

The steady-state current associated with the $(\text{BV-Q-BV}^{6+})_n$ -connected microelectrodes can be used to estimate^{14a,23} a range for D_{CT} for $(\text{BV-Q-BV}^{6+})_n$, assuming a concentration of charge-carrying redox centers between 0.8 and 2.4 M. A value of D_{CT} for poly(vinylferrocene) connecting a microelectrode array has recently been reported from this laboratory,^{14a} and Murray and co-workers have recently reported a D_{CT} value for a $\text{Ru}(\text{bpy})_3^{2+}$ -based polymer.^{23a} Equation 12 relates the steady-state

$$i = nFAD_{\text{CT}}C/d \quad (12)$$

current, i , the cross-sectional area of the polymer through which charge passes, A , the concentration of charge-carrying centers, C , the distance, d , across which charge must pass, n , F , and D_{CT} .²³ Calculating D_{CT} also requires knowing the proper value of n relevant to the BV-Q-BV^{6+} system. For reasons developed above we shall assume that $\text{BV}^{2+/+}$ self-exchange is the dominant mechanism for charge transport at low pH's and $n = 1$. For such assumptions Table III gives D_{CT} values determined under a wide range of conditions. The data for all entries in Table III assumes $C = 1.6$ M. As shown by the data in Table III, there is a pH dependence, like that illustrated in Figure 7, in 1 M LiCl as the electrolyte, but the effect is only about ~ 15 – 25% increase in D_{CT}

(23) (a) Chidsey, C. E. D.; Feldman, B. J.; Lundgren, C.; Murray, R. W. *Anal. Chem.* **1986**, *58*, 601. (b) Pickup, P. G.; Murray, R. W. *J. Am. Chem. Soc.* **1983**, *105*, 4510.

TABLE III: Values of D_{CT} and $D_{CT}C^2$ for $(BV-Q-BV^{6+})_n$ at 25 °C from Potential-Step and Steady-State Experiments

polymer	electrolyte/buffer ^a	pH	D_{CT} , cm ² /s × 10 ¹⁰		E_a , kJ/mol
			[$D_{CT}C^2$, mol ² s ⁻¹ cm ⁻⁴ × 10 ¹⁶]	potential step ^c	
$(BV^{2+})_n$ ^d	1 M LiCl/Tris	7-9	72.8 [352]	16.1 [78.0]	33.1
	0.5 M NaOTs/Tris	7-9	52.5 [254]		51.0
$(BV-Q-BV^{6+})_n$	1 M LiCl/Tris	7.2	2.7 [6.8]	0.8 [2]	49.0
	1 M LiCl/Tris	9.0	3.0 [7.7]		
	0.5 M NaOTs/acetate	6.0	4.1 [10.4]		
	0.5 M NaOTs/Tris	7.2	4.7 [12.0]		59.4
	0.5 M NaOTs/Tris	8.1	6.3 [16.0]		
	0.5 M NaOTs/Tris	9.0	8.8 [22.4]		60.3

^a All solutions contain 10% CH₃CN or *N,N*-dimethylformamide to suppress H₂ evolution. ^b Steady-state, generation/collection experiments using a polymer-coated microelectrode array with a microelectrode spacing of ~0.3 μm. The determination of D_{CT} from microelectrode assumes $C = 1.6$ M for $(BV-Q-BV^{6+})_n$ and $C = 2.2$ M for $(BV^{2+})_n$. ^c Potential-step experiment, 0.0 to -0.7 V vs SCE, for a polymer-coated platinum electrode. $D_{CT}C^2$ is a direct result from the measurement, and D_{CT} is calculated by assuming $C = 1.6$ M for $(BV-Q-BV^{6+})_n$ and $C = 2.2$ M for $(BV^{2+})_n$. ^d Data from ref 25.

upon increasing the pH. Note that the sodium tosylate electrolyte gives a larger value of D_{CT} and a larger pH dependence. A microelectrode coated with $(BV^{2+/+})_n$ from III shows the opposite dependence of D_{CT} on electrolyte; i.e., D_{CT} is lower for sodium tosylate vs LiCl, presumably due to the fact that tosylate is a bulkier, less mobile anion than Cl⁻. These data suggest that, for $(BV-Q-BV^{6+})_n$, anion mobility is not the limiting factor in determining the charge-transport rate and that other factors must be considered. Generator/collector experiments with microelectrodes connected with $(BV^{2+/+})_n$ have also shown that there is no pH dependence of D_{CT} over the range where the $(BV-Q-BV^{6+})_n$ polymer shows a marked pH dependence. Potential-step experiments can be used to determine $D_{CT}C^2$ for the electrode-bound $(BV-Q-BV^{6+})_n$ without direct evaluation of C .²⁴ Such a measurement gives a value of $D_{CT}C^2$ that is about the same as that obtained in the steady-state experiments with the microelectrodes. In 1.0 M aqueous LiCl, pH 7.2 (Tris), with 10% by volume CH₃CN (to suppress H₂ evolution) the potential-step method gives a value of $D_{CT}C^2 = 2 \times 10^{-16}$ mol²/(s cm⁴) under conditions where the steady-state generator/collector experiments give 6.8×10^{-16} mol²/(s cm⁴), assuming $C = 1.6$ M. Under the same conditions $D_{CT}C^2 = 7.8 \times 10^{-15}$ mol²/(s cm⁴) has been reported for $(BV^{2+/+})_n$ from III.³

The increase in the value of $D_{CT}C^2$ for higher pH's is likely due to a role for the cross redox process represented by (4). Effectively, the concentration of charge-carrying species can be increased by bringing the $E^{o'}$ for the Q/QH₂ centers to about the same value as that for the $BV^{2+/+}$ centers. Apparently, the cross-reaction rate constants are large enough to improve the steady-state charge-transport rate. Interestingly, the magnitude of the change in steady-state current passing through the $(BV-Q-BV^{6+})_n$ upon varying the pH from 6 to 9 is consistent with the magnitude of the concentration change in charge-carrying redox centers. Data obtained at pH 10 should show that the current declines, consistent with movement of $E^{o'}$ of the Q/QH₂ centers to an even more negative position than $BV^{2+/+}$. Unfortunately, the pH 10 data are not reliable, owing to loss of polymer (*vide supra*). The data for pH 6-9 is reproducible; data for pH <5 is difficult to obtain, owing to H₂ evolution from the microelectrodes at the negative potentials needed to reduce the BV^{2+} centers.

From the discussion above, the low-pH data are consistent with charge transport in the $(BV-Q-BV^{6+})_n$ system via a $BV^{2+/+}$ self-exchange path that is slower than in $(BV^{2+/+})_n$ from III. The "apparent" D_{CT} for $(BV-Q-BV^{6+})_n$ does increase at higher pH's due to the participation of Q centers in charge transport. If we assume that the participation of Q is only via the cross redox process represented by (4) and not via the self-exchange of Q centers according to (8), then it is evident that the cross redox process between the $(BV^{2+/+})$ and Q/QH₂ systems is about as important as $BV^{2+/+}$ self-exchange in charge transport at a pH where the $E^{o'}$'s of the two systems are similar. In essence, the

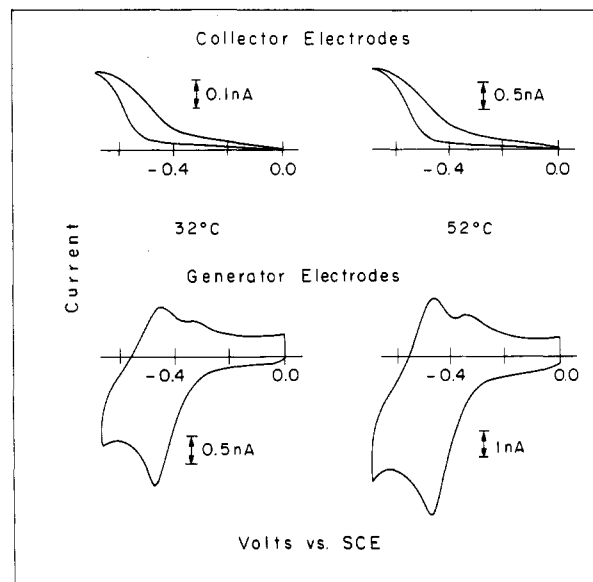
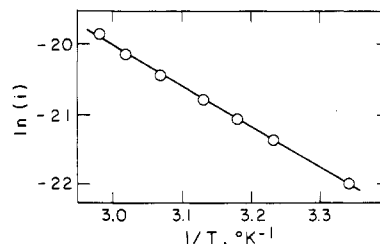


Figure 9. Temperature dependence of steady-state charge transport between generator electrodes (1, 3, 5, 7) and collector electrodes (2, 4, 6, 8) of the $(BV-Q-BV^{6+})_n$ -coated microelectrode array shown in Figure 6 and sketched in Scheme V. Data shown are for pH 7.2 (Tris)/1.0 M LiCl aqueous solution.

$(BV-Q-BV^{6+})_n$ polymer behaves as a diluted $(BV^{2+/+})_n$ polymer at low pH, with respect to steady-state charge-transport properties. The low values of $D_{CT}C^2$ for $(BV-Q-BV^{6+})_n$ vs $(BV^{2+})_n$ can thus be regarded partially as a consequence of the lower concentration of charge-carrying species 0.8-1.6 M vs 2.2 M. There is also the possibility that the BV^{2+} centers in $(BV-Q-BV^{6+})_n$ are further apart than in $(BV^{2+})_n$, but since the polymer is formed via hydrolysis of $-Si(OMe)_3$ on the BV^{2+} centers, it is not clear that the BV^{2+} - BV^{2+} separation in $(BV-Q-BV^{6+})_n$ will be greater. Further, the spectroscopic data appear to show $BV^+ - BV^+$ interaction.

Figure 9 illustrates the temperature dependence of the steady-state charge transport for $(BV-Q-BV^{6+})_n$ determined by using the generator/collector technique associated with a $(BV-Q-BV^{6+})_n$ -coated microelectrode array. The data shown are for pH 7.2, but essentially the same temperature dependence is found at pH 9. The plot of the log of the steady-state current, $\ln i$, vs

(24) Daum, P.; Lanhard, J. R.; Rolison, D.; Murray, R. W. *J. Am. Chem. Soc.* 1980, 102, 4649.

T^{-1} is a straight line and gives an Arrhenius activation energy of ~ 60 kJ/mol. The lack of a significant pH dependence on the activation energy is somewhat surprising considering that the cross redox process, (4), is apparently an important contributor to charge transport at high pH and would be expected to have activation parameters which are different from $BV^{2+/+}$ self-exchange. The pH independence suggests activation energy is associated with polymer motion rather than with fundamental rate constants associated with the charge-exchange processes. The activation energy for charge transport in $(BV-Q-BV^{6+})_n$ is somewhat larger than for that in $(BV^{2+})_n$ ^{3c,25} but in each case the activation energy depends on the electrolyte.

Conclusions

Electrochemical and optical measurements show that electrodes modified with $(BV-Q-BV^{6+})_n$ from I exhibit pH-dependent rectification. Studies of the electrochemistry of (Q/QH_2) from V show that the Q subunits in $(BV-Q-BV^{6+})_n$ are not capable of transporting charge through the polymer, owing to low rates of Q/QH_2 self-exchange. Electrochemical reduction of solution Q from VI by electrodes modified with $(BV^{2+})_n$ from III shows that the cross reaction $2BV^+ + Q + 2H^+ \rightarrow 2BV^{2+} + QH_2$ can occur with a large rate constant, establishing the viability of delivery of charge to the Q centers in $(BV-Q-BV^{6+})_n$ via the reduction of the BV^{2+} centers. Steady-state charge transport through $(BV-QH_2-BV^{6+})_n$ can occur via $BV^{2+/+}$ self-exchange, but the value of D_{CT} is much smaller than that for $(BV^{2+/+})_n$ from III. Nonetheless, the $BV^{2+/+}$ self-exchange provides a path to effect electrochemical reduction of all Q centers in $(BV-Q-BV^{6+})_n$ even at coverages in excess of 10^{-8} mol/cm². Thus, pH-dependent rectification for electrodes modified with $(BV-Q-BV^{6+})_n$ is due to a combination of kinetic and thermodynamic factors: (i) the bulk of the Q centers are not directly electrochemically accessible due to the poor kinetics for the Q/QH_2 self-exchange process, (ii) the Q centers are rapidly reducible to QH_2 via reaction with BV^+ , and (iii) the QH_2 centers cannot return charge to the electrode via the $BV^{2+/+}$ system at low pH's, because the $E^{\circ'}$ values show that the reduction of BV^{2+} by QH_2 is not thermodynamically viable.

An electrode modified with a bilayer assembly^{6,7} of $(BV^{2+})_n/(Q)_n$ formed by first derivatization with III followed by reaction with V, shows pH-dependent rectification as would be expected: at high pH where the $E^{\circ'}$'s of $(BV^{2+/+})$ and $(Q/QH_2)_n$ are similar, reversible reduction of the assembly occurs, $(BV^{2+})_n/(Q)_n \rightleftharpoons (BV^+)_n/(QH_2)_n$, but at low pH where QH_2 is incapable of reducing BV^{2+} centers, the reduction of Q to QH_2 cannot be reversed. However, unlike the $(BV-Q-BV^{6+})_n$ assembly, the reduction of $(BV^{2+})_n/(Q)_n$ does not result in reduction of all Q centers to QH_2 at low pH because charge transport in the $(Q/QH_2)_n$ outer layer is too sluggish. Accordingly, the "homogeneous" bilayer $(BV-Q-BV^{6+})_n$ allows a larger absolute amount of charge trapping than can be obtained in a conventional bilayer assembly like $(BV^{2+})_n/(Q)_n$.

There is a relatively modest change in the steady-state charge-transport properties of $(BV-Q-BV^{6+})_n$ as a function of pH. From the magnitude of the effect it is concluded that the cross exchange between $BV^{2+/+}$ and Q/QH_2 can contribute to the overall charge transport in the polymer to increase " D_{CT} " at pH's where the cross-reaction rate is significant. The intrinsic pH-dependent charge transport in a redox polymer could, in principle, be exploited to make a pH sensor, but the magnitude of the dependence would seem to be too modest for practical applications. Indeed, the intrinsic properties of the $(Q/QH_2)_n$ system itself would appear to be more useful in this regard.^{26,27}

The fundamental finding of interest in connection with the $(BV-Q-BV^{6+})_n$ system is the fact that rectification is achievable.

The leading factors that bring about rectification are summarized above. A factor that has not been discussed is structure. The optical spectroscopy of II in solution shows evidence for BV^+-BV^+ interaction even in very dilute solutions. Such intramolecular interactions make possible electron exchange between the BV^+ centers. The $-Si(OMe)_3$ groups in the para position of the terminal phenyl rings in I suggest formation of a siloxane polymer where the BV^{2+} centers of adjacent repeat units in $(BV-Q-BV^{6+})_n$ will be able to interact as do the BV^{2+} centers in $(BV^{2+})_n$ from III. The optical spectroelectrochemistry of $(BV-Q-BV^{6+})_n$ is consistent with interaction between the BV^+ centers, based on the position of the visible absorption maximum for the reduced $(BV^+-containing)$ polymer compared to site-isolated BV^+ centers. There is no clear structural feature responsible for slow charge transport via $BV^{2+/+}$ self-exchange in $(BV-Q-BV^{6+})_n$ compared to $(BV^{2+})_n$. However, the higher activation energy for charge transport, the differing electrolyte effects on D_{CT} , and the penetration of $Ru(NH_3)_6^{3+}$ through $(BV-Q-BV^{6+})_n$, all signal significant structural differences between $(BV-Q-BV^{6+})_n$ from I and $(BV^{2+})_n$ from III.

The ability to observe rectification at very low coverages of $(BV-Q-BV^{6+})_n$ is likely due to the fact that structural constraints preclude direct electrode access to all Q centers. As the data in Figure 1 clearly show, there are some Q centers that are directly electrode accessible and these behave like Q centers from surface-confined material from V. However, it is noteworthy that rectification is observed at coverages of $(BV-Q-BV^{6+})_n$ which are significantly lower than coverages of $(Q)_n$ from VI where all Q centers are electrochemically accessible. This fact suggests that the structural arrangement of the redox subunits is critical to achieving rectification.

The not surprising conclusion that structure is crucial means that rational design of molecular systems for unidirectional electron transfer will require input regarding the structure dependence of the rate of electron transfer between molecular subunits in an electrode-confined molecular assembly. It is appreciated that impressive progress is emerging from studies of multicomponent molecules in solution involving a variety of modified biological systems²⁸⁻³⁰ and purely man-contrived synthetic assemblies.³¹⁻³³ Extending these studies to systems anchored to conductors for application in photoconversion, sensors, and molecular electronics is possible.²⁷ It is noteworthy that studies of energy and electron transfer in multilayer assemblies fabricated by Langmuir-Blodgett techniques³⁴ show promise for producing highly ordered, multicomponent, molecular assemblies. Further, deliberate synthesis of macromolecular assemblies of known structure that can be covalently anchored to conductors in a known orientation should be possible.

Acknowledgment. We thank the U.S. Department of Energy, Office of Basic Energy Sciences, Division of Chemical Sciences, for support of this research. We also gratefully acknowledge use of the Central Facilities of the MIT Center for Materials Science and Engineering.

Registry No. I, 112818-42-5; I (homopolymer), 112795-44-5; II, 112818-39-0; V, 112818-40-3; VI, 112818-41-4; VII, 112818-33-4; VI-IIa(R'=H), 85578-06-9; VIIIB(R'=Si(OMe)₃), 112818-34-5; IXa(R'=H), 112818-36-7; IXb(R'=Si(OMe)₃), 112818-38-9; Me₂N(CH₂)₂NH₂, 108-00-9; C₆H₅CH₂Cl, 100-44-7; 4-(MeO)₃SiC₆H₄CH₂Cl, 24413-04-5; 4-BrCH₂C₆H₄CH₂Br, 623-24-5; tetrachloro-1,4-benzoquinone, 118-75-2; 4,4'-bipyridine, 553-26-4.

(28) Mayo, S. L.; Ellis, W. R.; Crutchley, R. J.; Gray, H. B. *Science (Washington, DC)* **1986**, *233*, 948, and references cited therein.

(29) McClendon, G.; Miller, J. P. *J. Am. Chem. Soc.* **1985**, *107*, 7811, and references cited therein.

(30) Liang, N.; Kang, C. H.; Margoliash, E.; Shing, H. P.; Hoffman, B. M. *J. Am. Chem. Soc.* **1986**, *108*, 4665, and references cited therein.

(31) Jorvan, A. D.; Leland, B. A.; Geller, G. G.; Hopfield, J. J.; Dervan, P. B. *J. Am. Chem. Soc.* **1984**, *106*, 6090, and references cited therein.

(32) Wasielewski, M. R.; Niemczyk, M. P.; Svec, W. A.; Dewitt, E. B. *J. Am. Chem. Soc.* **1985**, *107*, 5562, and references cited therein.

(33) Miller, J. R.; Calcuterra, L. T.; Closs, G. L. *J. Am. Chem. Soc.* **1984**, *106*, 3047, and referenced cited therein.

(34) (a) Kuhn, H. *Pure Appl. Chem.* **1979**, *51*, 341. (b) Mobius, D. *Acc. Chem. Res.* **1981**, *14*, 63.

(25) Lane, G. A.; Lewis, T. J.; Wrighton, M. S., to be submitted.

(26) Wrighton, M. S.; Thackeray, J. W.; Natan, M. J.; Smith, D. K.; Lane, G. A.; Belanger, D. *Philos. Trans. R. Soc. London, B* **1987**, *316*, 13.

(27) Wrighton, M. S. *Comments Inorg. Chem.* **1985**, *4*, 269.